Original Contribution

Kurume Medical Journal, 55, 37-41, 2008

Endoscopic Sinus Surgery for the Treatment of Organized Hematoma of the Maxillary Sinus

HIDEAKI SUZUKI, TSUYOSHI INABA, NOBUAKI HIRAKI, KOICHI HASHIDA, TETSURO WAKASUGI, YOHEI KADOKAWA AND TSUYOSHI UDAKA

Department of Otorhinolaryngology, School of Medicine, University of Occupational and Environmental Health, Kitakyushu 807-8555, Japan

Received 3 July 2008, accepted 30 September 2008

Edited by TADASHI NAKASHIMA

Summary: Organized hematoma is a benign and non-neoplastic lesion, however, differential diagnosis from neoplastic diseases is always problematic, and patients are often forced to sustain excessive surgical invasion. We retrospectively studied the characteristics of imaging findings of organized hematoma of the maxillary sinus, and estimated the validity and effectiveness of endoscopic sinus surgery for the treatment of this disease. Three patients (2 men and a woman, ranging in age from 50 to 62 years) with organized hematoma of the maxillary sinus who underwent endoscopic sinus surgery were retrospectively analyzed. The diagnosis was provisionally made based on the findings of preoperative computed tomography (CT) and magnetic resonance imaging (MRI), and was confirmed by histopathological examinations of surgical specimens. CT revealed a well-defined expansile mass in the unilateral sinus associated with thinning and expansion of the medial sinus wall in all the cases. On contrast-enhanced images, patchy heterogeneous enhancement was observed. Intermingled low/intermediate/high signal intensity was seen on both T1- and T2-weighted MRI. The lesions were curetted via an endoscopic middle meatal antrostomy with the assistance of a microdebrider. None of the patients received arterial embolization or blood transfusion. Histopathological findings were consistent with those of organized hematoma. Their postoperative courses were uneventful, and all the patients are currently free from disease. We conclude that organized hematoma of the maxillary sinus can be successfully treated by endoscopic sinus surgery under accurate preoperative diagnosis and careful surgical planning.

Key words organized hematoma, maxillary sinus, endoscopic sinus surgery, microdebrider, computed tomography, magnetic resonance imaging

INTRODUCTION

Organized hematoma is a benign hematoma-like pseudotumor, which preferably arises in the maxillary sinus. Less frequently, such a lesion may arise from the pericardium, cerebrum, adrenal gland, cerebellopontine angle, etc. Organized hematoma of the maxillary sinus was first described by Tadokoro [1] in 1917 in the Japanese literature. The occurrence of this disease has also been sporadically documented in the English literature in the 1990s and 2000s [2-10]. Although the disease is essentially benign and non-neoplastic, differential diagnosis from neoplastic diseases including malignancy has been always problematic, and patients have been often forced to sustain excessive surgical invasion. In recent years, however, indication of endoscopic surgery is increasing for the treatment of this disease under precise preoperative

Corresponding author: Hideaki Suzuki, M.D., Ph.D., Department of Otorhinolaryngology, School of Medicine, University of Occupational and Environmental Health, 1-1 Iseigaoka, Yahatanishi-ku, Kitakyushu 807-8555, Japan. Tel: +81-93-691-7448 Fax: +81-93-601-7554 E-mail: suzuhyde@med.uoeh-u.ac.jp

Abbreviations: CT, computed tomography; MRI, magnetic resonance imaging.

imaging examinations. We herein studied the characteristics of imaging findings of organized hematoma of the maxillary sinus, and estimated the validity and effectiveness of endoscopic sinus surgery for the treatment of this disease.

PATIENTS AND METHODS

Three patients with organized hematoma of the maxillary sinus who were treated in our department from 2004 to 2006 were retrospectively analyzed on the basis of their medical records. They were 2 men and a woman, ranging in age from 50 to 62 years. The diagnosis was provisionally made from the findings of preoperative computed tomography (CT) and magnetic resonance imaging (MRI), and was confirmed by histopathological examinations of surgical specimens.

RESULTS

The patients' clinical features are summarized in Table 1. The chief complaints were nasal obstruction, nasal bleeding, and bloody rhinorrhea. None had a past history of nasal or paranasal sinus surgery. Two patients were receiving anticoagulant drugs for the treatment of underlying diseases. These drugs were halted during the perioperative period. On anterior rhinoscopy, the lateral nasal wall was medially displaced in cases 1 and 3, and a blood clot was seen in the middle nasal meatus in case 2. CT revealed a well-defined expansile mass in the unilateral sinus associated with thinning and expansion of the medial sinus wall in all the cases (Fig. 1). On contrast-enhanced images, patchy heterogeneous enhancement was observed (Fig. 2). The lesions showed intermingled low/intermediate/high signal intensity on both T1- and T2-weighted MRI (Fig. 3). From these findings, we suspected that the lesions were probably organized hematomas. Because contrast enhancement was only patchy, preoperative arterial embolization was not performed in any of the cases. Macroscopically, a dark-reddish crumbly lump consisting of blood clots and fibrous tissue filled the sinus of each patient. The lesions were curetted by

TABLE 1.
Summary of patients' profile

Case	Age/Sex	Side	Chief complaint	Underlying disease	Anticoagulant drug	Total blood loss during surgery	Operation time
1	62/M	R	Nasal bleeding Nasal obstruction	Old myocardial infarction	Warfarin	250 ml	80 min
2	50/F	L	Bloody rhinorrhea	Anorexia nervosa	(–)	250 ml	70 min
3	57/M	L	Nasal obstruction	Ischemic heart disease	Aspirin	350 ml	110 min

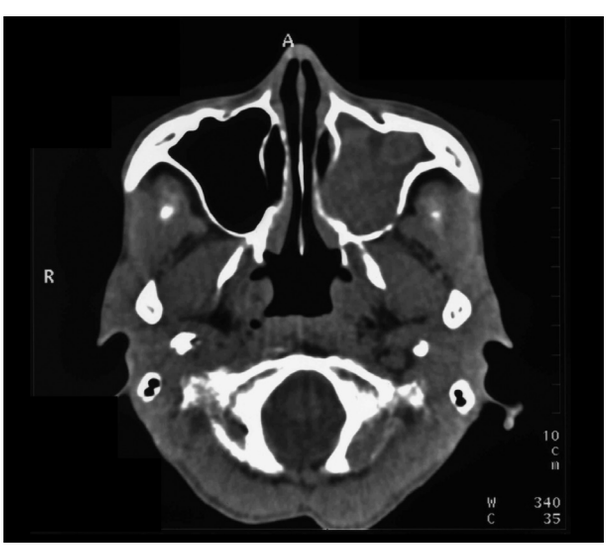

Fig. 1. Plain CT of case 2 showing a well-defined expansile mass in the left maxillary sinus.

Fig. 2. Contrast-enhanced CT of case 2 showing patchy heterogeneous enhancement.

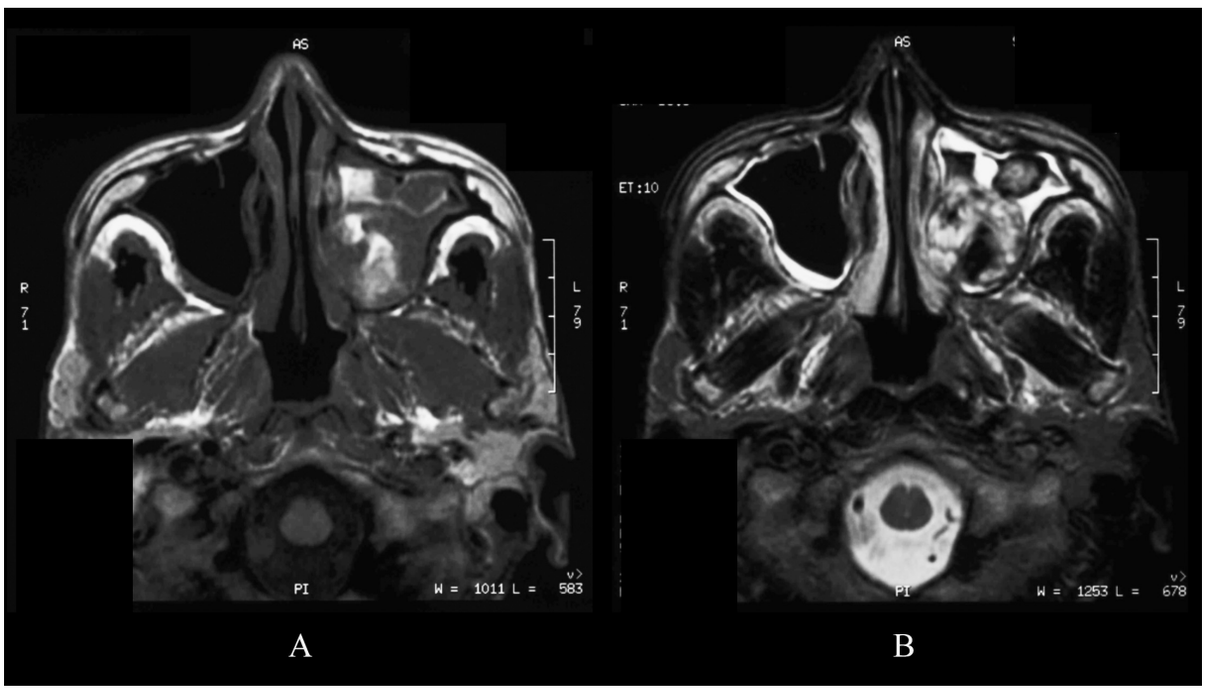

Fig. 3. MRI of case 2. The lesion shows intermingled low/intermediate/high signal intensity on both T1- (A) and T2- (B) weighted MRI.

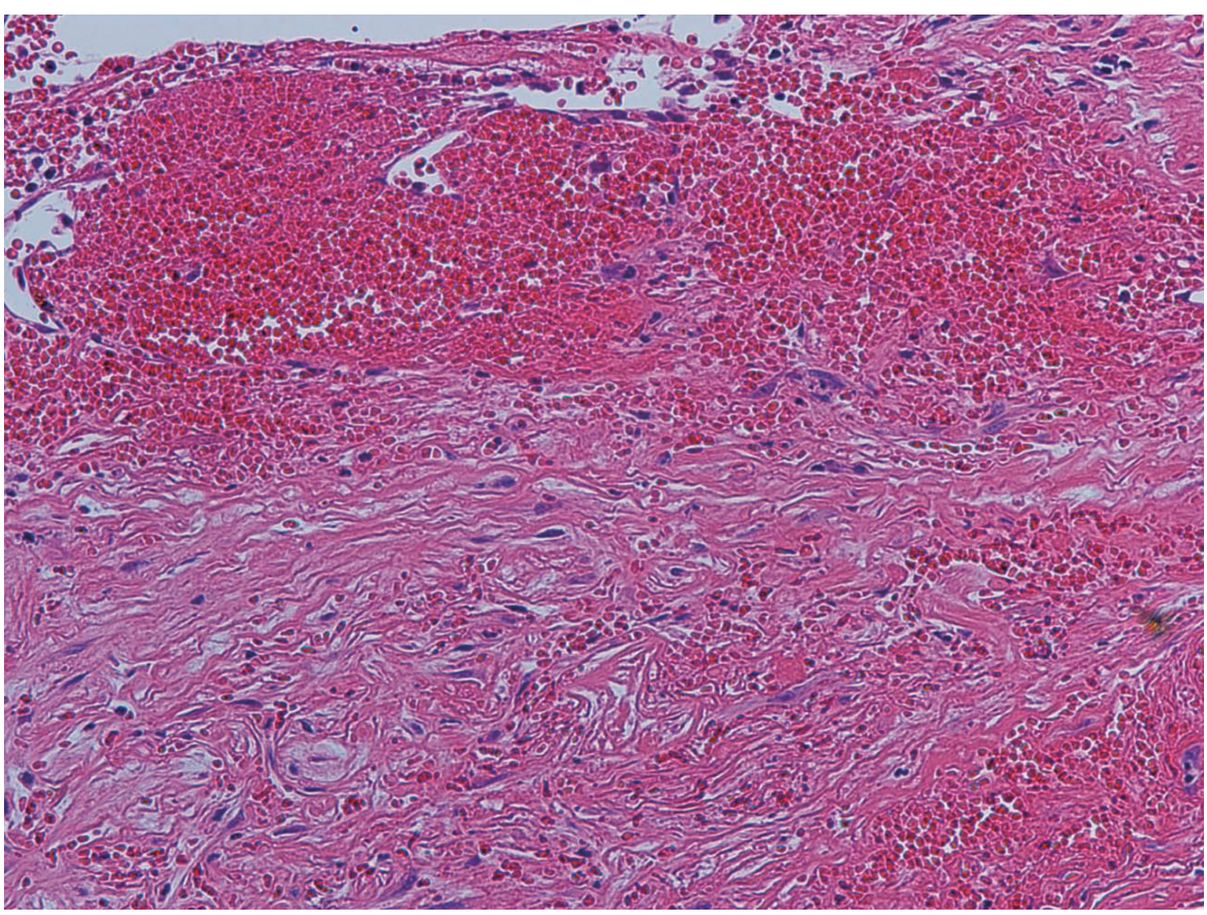

Fig. 4. Photomicrograph of case 2. The lesion comprises hemorrhage and blood clots coexisting with neovascularization and fibrosis without evidence of neoplasm. (H & E stain, original magnification ×200)

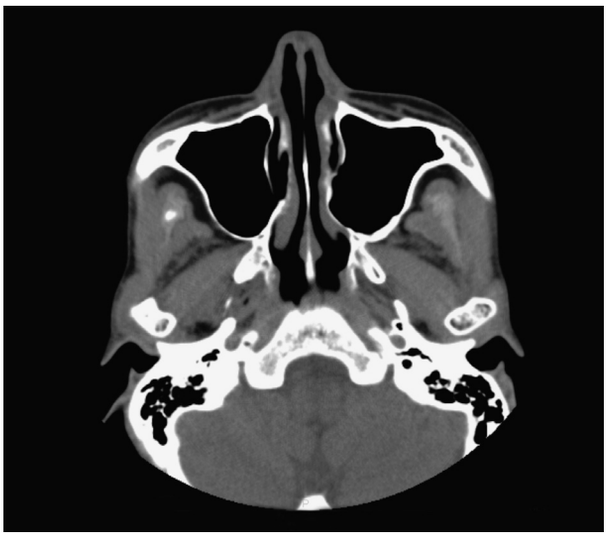

Fig. 5. Postoperative CT of case 2. The sinus is completely clear 16 months after surgery.

piecemeal via endoscopic middle meatal antrostomy with the assistance of a microdebrider. In case 2, the mass was broadly based on the lateral wall of the sinus, whereas the other portion of the mass was readily separated from the sinus mucosa. In the other cases, no obvious base was seen, and the border between the lesion and sinus mucosa was endoscopically unclear. The lesions were eradicated as thoroughly as possible, but small remaining tissue was left, particularly, on the anterior and inferomedial walls in the sinus. Total blood losses during surgery were 250-350 ml, and no blood transfusions were needed. Operation times were 70-110 min. Intraoperative frozen-section analysis was performed in 2 patients, showing consistent findings with those of organized hematoma and no evidence of malignancy. In the other patient (case 2), an almost definite diagnosis was preoperatively obtained from typical radiographic findings, and thus, an intraoperative pathology consultation was not arranged. Microscopically, the lesions comprised hemorrhage and blood clots coexisting with neovascularization and fibrosis without evidence of neoplasms (Fig. 4). Their postoperative clinical courses were uneventful, and all the patients are free from disease 2-4 years after surgery (Fig. 5).

DISUCUSSION

Since organized hematoma of the maxillary sinus was first described by Tadokoro [1] in 1917, a number of authors have reported this disease in the Japanese literature. On the other hand, in the English literature, there are only few papers on this disease. A case report by Ozhan et al. [2] in 1996 is the first English document about organized hematoma of the maxillary sinus, which was associated with von Willebrand's disease. At a later time, in the 2000s, organized hematoma of the maxillary sinus was reported in patients without bleeding diathesis [3], and was recognized to often be an idiopathy. This disease has been otherwise referred to as hemophilic pseudotumor [2] or a hematoma-like mass [6], but the term "organized hematoma" is most commonly accepted [3,5,7-10].

It is important to read the characteristics of imaging in order to make an unerring preoperative diagnosis. On CT, an organized hematoma generally exhibits a well-defined expansile mass in the unilateral sinus often associated with thinning or resorption of the surrounding bone. The medial sinus wall, particularly the uncinate process, is most frequently eroded, and resorption of the posterior, superior and anterior sinus wall is sometimes observed [8]. The lesion may show heterogeneous X-ray density, but calcification is rarely seen. No bilaterally-affected case has been reported to date. On contrast-enhanced images, enhancement is usually patchy and heterogeneous [7-10], but may occasionally be faint and unremarkable [2-4]. More conspicuous characteristics are seen on MRI. The lesion has a clear contour often surrounded by edematous sinus mucosa, and shows intermingled heterogeneous low/intermediate/high signal intensity on both T1- and T2-weighted MRI [2,6,9,10].

Because the clinical and radiographic appearance of organized hematoma is similar to that of neoplasms such as hemangioma, papilloma, schwannoma, carcinomas, sarcomas, and lymphoma, most of the previous cases have undergone surgical resection via a Caldwell-Luc operation, Denker's operation, or a lateral rhinotomy approach. However, considering the benign and non-neoplastic nature of organized hematoma, a less invasive surgical approach is desirable. Recent reports have described an endoscopic approach to evacuating this lesion [5,7-9]. In the present patients, organized hematoma was curetted by piecemeal via endoscopic sinus surgery with the assistance of a microdebrider. The middle meatal approach may be insufficient for the access to the anterior and inferomedial walls of the sinus, and in the present cases, small remaining tissue was left behind in the sinus. However, the disease eventually cured in all the cases, indicating that combination with other approaches such as inferior meatal and transcanine antrostomy is basically unnecessary.

There are several requirements for the application

of endoscopic sinus surgery in order to achieve good treatment outcome of this disease: First, the preoperative diagnosis needs to be made as accurately as possible. The radiographic findings mentioned above give convincing clues for making a diagnosis. Second, if there is underlying bleeding diathesis, it must be thoroughly controlled. Even in patients without bleeding disorders, organized hematoma may still be hemorrhagic, but the lesion generally shows only weak and patchy enhancement, as in the present study. Preoperative arterial embolization has not been performed in the reported or present cases, and is thought to be unnecessary. Third, intraoperative frozen-section analysis is advisable because the preoperative diagnosis is often in doubt. If neoplasms including malignancy are suspected by pathology consultation, other surgical procedures such as a Caldwell-Luc operation, Denker's operation, midfacial degloving or a lateral rhinotomy approach should be immediately indicated. Fourth, the use of a microdebrider is strongly recommended in combination with an endoscopic approach for the evacuation of the maxillary sinus, particularly, the anterior and inferomedial portions of the sinus.

CONCLUSION

We retrospectively studied the characteristics of imaging findings of organized hematoma of the maxillary sinus, and estimated the validity and effectiveness of endoscopic sinus surgery for the treatment of this disease. We would like to emphasize that this disease can be successfully treated via an endoscopic approach. Accurate preoperative diagnosis and careful surgical planning play key roles in attaining this goal.

REFERENCES

1. Tadokoro K. Jogakudo ketsuryu ni tsuite. Dainichijibi 1917; 23:359-360. (in Japanese)
2. Ozhan S, Arac M, Isik S, Oznur II, Atilla S et al. Pseudotumor of the maxillary sinus in a patient with Von Willebrand's disease. Am J Roentgenol 1996; 166:950-951.
3. Unlu HH, Mutlu C, Ayhan S, and Tarhan S. Organized hematoma of the maxillary sinus mimicking tumor. Auris Nasus Larynx 2001; 28:253-255.
4. Tabaee A, and Kacker A. Hematoma of the maxillary sinus presenting as a mass–a case report and review of literature. Ont J Pediatr Otorhinolaryngol 2002; 65:153-157.
5. Lee BJ, Park HJ, and Heo SC. Organized hematoma of the maxillary sinus. Acta Otolaryngol 2003; 123:869-872.
6. Yagisawa M, Ishitoya J, and Tsukuda M. Hematoma-like mass of the maxillary sinus. Acta Otolaryngol 2006; 126:277-281.
7. Yoon TM, Kim JH, and Cho YB. Three cases of organized hematoma of the maxillary sinus. Eur Arch Otorhinolaryngol 2006; 263:823-826.
8. Lee HK, Smoker WR, Lee BJ, Kim SJ, and Cho KJ. Organized hematoma of the maxillary sinus: CT findings. Am J Roentgenol 2007; 188:W370-W373.
9. Shen KJ, Som PM, and Teng MS. Radiology quiz case 2. organized hematoma of the maxillary sinus. Arch Otolaryngol Head Neck Surg 2007; 133:408-410.
10. Nishiguchi T, Nakamura A, Mochizuki K, Tokuhara Y, Yamane H et al. Expansile organized maxillary sinus hematoma: MR and CT findings and review of literature. Am J Neuroradiol 2007; 28:1375-1377.

Original Contribution

Kurume Medical Journal, 55, 43-53, 2008

3D Anatomical Variations of Hepatic Vasculature and Bile Duct for Right Lateral Sector of Liver with Special Reference to Transplantation

ATSUSHI YOSHIDA, KOJI OKUDA, HISAMUNE SAKAI, HISAFUMI KINOSHITA AND SHIGEAKI AOYAGI

Department of Surgery, Kurume University School of Medicine, Kurume 830-0011, Japan

Received 6 November 2008, accepted 4 February 2009

Edited by MICHIO SATA

Summary: To achieve a safer living related liver transplantation (LRLT) using the right lateral sector, anatomical variations of the portal vein, hepatic artery and bile duct for the right lateral sector and their three dimentional (3D) relationship were assessed by integrated 3D-CT images. 52 patients who underwent contrast enhanced multidetector row CT (MD-CT) and MD-CT cholangiography were enrolled. Data from contrast enhanced MD-CT were used to reconstruct the 3D images of the hepatic artery and portal vein. 3D images reconstructed from MD-CT data of the hepatic artery, portal vein and bile duct were integrated into a single image. The dual branching of the right lateral portal vein was observed in 22 (42.3%) patients. Three (5.8%) had dual right lateral ducts and 14 (26.9%) had dual right lateral arteries. Among them, "south-turning" artery and "north-turning" bile duct was observed in 22 (42.3%). "South-turning" artery and "south-turning" bile duct were 3 (5.8%). "North-turning" artery and "north-turning" bile duct were 2 (7.4%). Only 27 (51.9%) had single portal vein, bile duct and artery for the right lateral sector, those were preferable as candidates for right lateral sector graft transplantation. 3D anatomical variations of portal vein, artery and bile duct for the right lateral sector were complexed, and only half of the donor candidates had preferable hepatic structures for right lateral sector graft transplantation. Understanding of the 3D hepatic structures by 3D-CT may contribute to a better definition of anatomical contraindications for LRLT which may further results in more safe and widely applied right lateral sector graft LRLT.

Key words liver transplantation, right lateral sector, MD-CT, 3D image

INTRODUCTION

Living related liver transplantation (LRLT) was initially introduced in pediatric patients [1], but recently it has been widely applied for adult patients because of the scarcity of cadaveric donors in Japan [2]. In adult-to-adult LRLT, small for size grafts are often transplanted because the resected liver volume is optimized for donor safety. Fan et al. [3] reported that safe donation is possible only when the estimated residual liver volume is over 30%. Leelaudomlipi et al. [4] indicated that 25% of the potential donors had a large right lobe which accounted for more than 70% of the whole liver volume. Therefore, the right lobe graft retrieval is not possible in all potential donors. In contrast, a left lobe graft usually does not satisfy the recipient metabolic demand [5]. To overcome this problem, a right lateral sector graft is newly introduced [6]. According to volumetric studies [4,7], in 9-18% of potential donors, the right lobe volume ex-

Corresponding author: Koji Okuda, Department of Surgery, Kurume University School of Medicine, 67 Asahi-machi, Kurume 830-0011, Japan. Tel: +81-942-35-3311 Fax: +81-942-35-8967 E-mail: kook@med.kurume-u.ac.jp

Abbreviations: DIC, drip infusion cholangiography; GDA, gastroduodenal artery; LHD, left hepatic duct; LLA, left lateral artery; LRLT, living related liver transplantation; MD-CT, multi-detector computed tomography; MHA, middle hepatic artery; PTBD, percutaneous transhepatic biliary drainage; RHA, right hepatic artery; RL, right lateral portal vein; RLA, right lateral artery; RLD, right lateral duct; RPM, right paramedian portal vein; RPMA, right paramedian artery; RPMD, right paramedian duct; SMA, superior mesenteric artery; 2D, two dimension/dimensional; 3D, three dimension/dimensional.

ceeds 70% of the total liver volume and the right lateral sector has a volumetric advantage than the left lobe.

However, it is obvious that the procurement of the right lateral sector has technical difficulties. Only a few centers are using the right lateral sector graft for transplantation [7,8-10]. The high number of either unrecognized or extemporaneously handled biliary and vascular variants pose high risk both to the donor and the recipient [11]. Preoperative understanding of the anatomical variations of the sectoral and the segmental bile ducts, the hepatic artery and the portal vein is essential to evaluate the feasibility of the right lateral sector transplantation, and to achieve safe transplantation.

Newly developed multi-detector computed tomography (MD-CT) images of the portal vein, the hepatic artery and the bile duct enable us to define the variations of the segmental hepatic structures accurately [12,13] and the three dimension (3D) integrated images contribute to surgical simulation in a better way.

This study was aimed to define the anatomical variations of the portal vein, the hepatic artery and the bile duct for the right lateral sector based on the integrated 3D images in order to help in framing the guidelines for transplantation.

MATERIALS AND METHODS

Patients

Between November 2002 and December 2006, 73 patients underwent contrast enhanced dynamic MD-CT and MD-CT cholangiography in our department, in ordinal clinical schedule for preoperative evaluation. After review these cases, 66 patients who met the following inclusion criteria were selected: age over 20 years, no tumor in the liver/hepatic hilum, no tumor located in peripheral sites in the liver which is more than 30mm in diameter, no previous hepatic or biliary surgery. 3D images of the portal vein, the hepatic artery and the bile duct were reconstructed in all. 14 patients were excluded from the study because of the poor quality of the 3D images. Consequently, 52 patients were enrolled in this study. There were 40 males and 12 females with age ranged from 42-78 (mean 65) years. The pathological diagnosis in these patients were as follows: hepatocellular carcinoma-24, cholangiocellular carcinoma-4, extrahepatic bile duct cancer-7, pancreatic cancer-3, papilla vater carcinoma-1, gall bladder cancer-5, adenomyomatosis-1, gall stones-5, chronic hepatitis-1 and liver hemangioma-1.

MD-CT protocol

All dynamic CT studies were performed with MD-CT (Asteon multi ver. 1.5 Toshiba, Tokyo or LightSpeed Plus, GE Yokogawa, Tokyo). Patients received 100 ml of iopamidol with an iodine concentration of 370 mg/ml (Iopamiron 370; Nihon Schering, Osaka, Japan) as intravenous contrast for vascular imaging. The contrast medium was injected at a rate of 4 ml/sec. with an automatic power injector. Three or four phase scanning was performed with a single breath-hold helical technique at 3 mm collimation, 3.5 helical pitch and 0.75 sec gantry rotation speed. Data from the artery dominant phase and the portal vein dominant phase were used to reconstruct the 3D images.

For biliary imaging, in 38 cases, CT scan images were acquired 30 min after the intravenous infusion of 100 ml of biliary contrast agent (Meglumine isotraxate, Biliscopin; Shering, Berlin, Germany) at a rate of 0.1 ml/sec. (DIC-CT). In all 38 cases, DIC-CT and dynamic CT scan were performed on different days. In 14 cases having a percutaneous transhepatic biliary drainage (PTBD) tube, biliary enhanced CT was performed after the administration of 3-15 ml of 6% biliary contrast agent (Meglumine sodium amidotrizoate, Urografin; Shering, Berlin, Germany) through the PTBD tube (PTBD-CT). The adequate volume of the contrast agent was determined by the previously performed PTBD cholangiography.

Image interpretation

Analysis of the image data was performed based on the source images and the 3D postprocessing images on commercially available workstations (Intage rvse, KGT, Tokyo and VertualPlace, AZE, Osaka). 3D reconstruction of the hepatic vasculature was made using a volume rendering algorithm. The volume rendered images were obtained in projections selected to depict the course of the hepatic vasculature best. The resulting 3D images of the hepatic artery, the portal vein and the bile duct rendered for each step of the artery dominant phase, the portal vein dominant phase and the DIC-CT/PTBD-CT respectively were carefully reviewed and compared with the axial source images to ensure that no important structure was inadvertently deleted from the 3D images. 3D images of the hepatic artery, the portal vein and the bile duct which were adjusted to position each other focusing at the hepatic hilum on 2D axillary, sagital and coronary

Fig. 1. Integrated image of the 3D portogram, angiogram and cholangiogram.

imaging sequences were further integrated into a single image (Fig. 1). To increase the accuracy, 3D images were reconstructed by three surgeons who are experts in hepatico-biliary anatomy and 3D reconstruction (A. Y., H. S and K. O with 8, 12 and 26 years of experience respectively). The study was regarded as diagnostic when both the biliary and the vascular structures were significantly enhanced to allow reliable determination or exclusion of anatomic variants especially in a surgical perspective.

In this study, anatomical variation of each of portal vein, artery and bile duct for the right lateral sector was investigated. Further, as it is important for operation to know the anatomical arrangement of the right hepatic duct/artery, the right paramedian segmental duct/artery and the right lateral segmental duct/artery in the hilar area [17], the 3D relationship of segmental hepatic duct/artery to portal vein was assessed. The segmental artery/bile duct branches which run and course to the dorsal and cranial side of the right paramedian portal vein are termed "north turning" artery/bile duct branch, and those which run and course to the ventral and caudal side of the portal vein are termed "south tuning" branch, as Kawarada et al. [17] named in the previous report. Intrahepatic structures are termed according by the Couinaud's terminology [14]. Namely, the right paramedian portal vein/artery and bile duct are corresponding to the right anterior portal vein/artery and bile duct in Zollinger's classification [15,16]. The right lateral portal vein/artery and bile duct are corresponding to the right posterior portal vein/artery and bile duct.

RESULTS

Diagnostic examination

In 52 of the 66 evaluated patients, the MD-CT studies were considered as diagnostic. The study was not diagnostic in the remaining 14 patients because of the poor timing of the contrast and the image acquisition. One patient had poor arterial phase images, 9 had poor biliary images and 4 had both. Portal imaging was satisfactory in all patients.

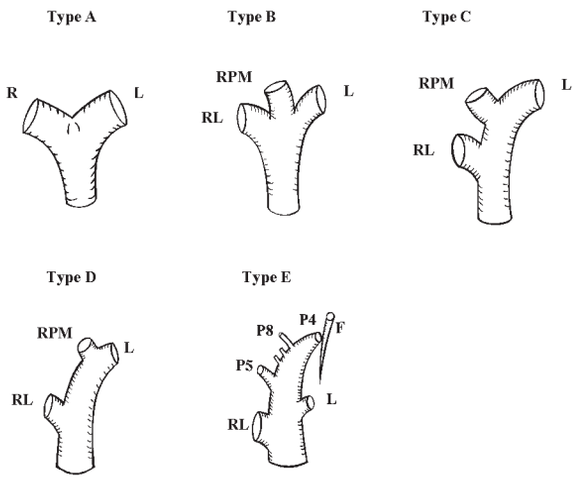

Fig. 2. Anatomical variant of portal vein.
Type A: 42 cases (80.8%), Type B: 3 cases (5.8%), Type C: 6 cases (11.5%), Type D : 1 case (1.9%), Type E : 0 cases (0%)
RPM: right paramedian portal vein, RL: right lateral portal branch, R: right portal vein, L: left portal vein, P5: portal vein for the segment 5, P8: portal vein for the segment 8, P4: portal vein for the segment 4, F: right sided round ligament

Analysis of the portal veins

Branching pattern of the right portal vein was defined into 5 types according to Nakamura's classification (Fig. 2) [18]. Standard anatomy with bifurcation of the main portal vein into left and right was seen in 42 patients (type A, 80.8%). Anatomical variations were observed in 10 patients. Trifurcation of the right paramedian portal vein (RPM), the right lateral portal

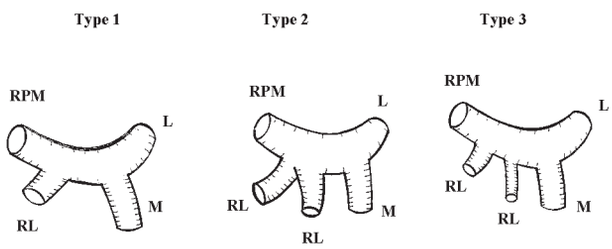

Fig. 3. Anatomical variant of right lateral portal vein.
Type 1: 30 cases (57.7%), Type 2: 10 cases (19.2%), Type 3: 12 cases (23.1%)
*RPM: right paramedian portal vein, RL: right lateral portal branch, M: main portal vein, L: left portal vein

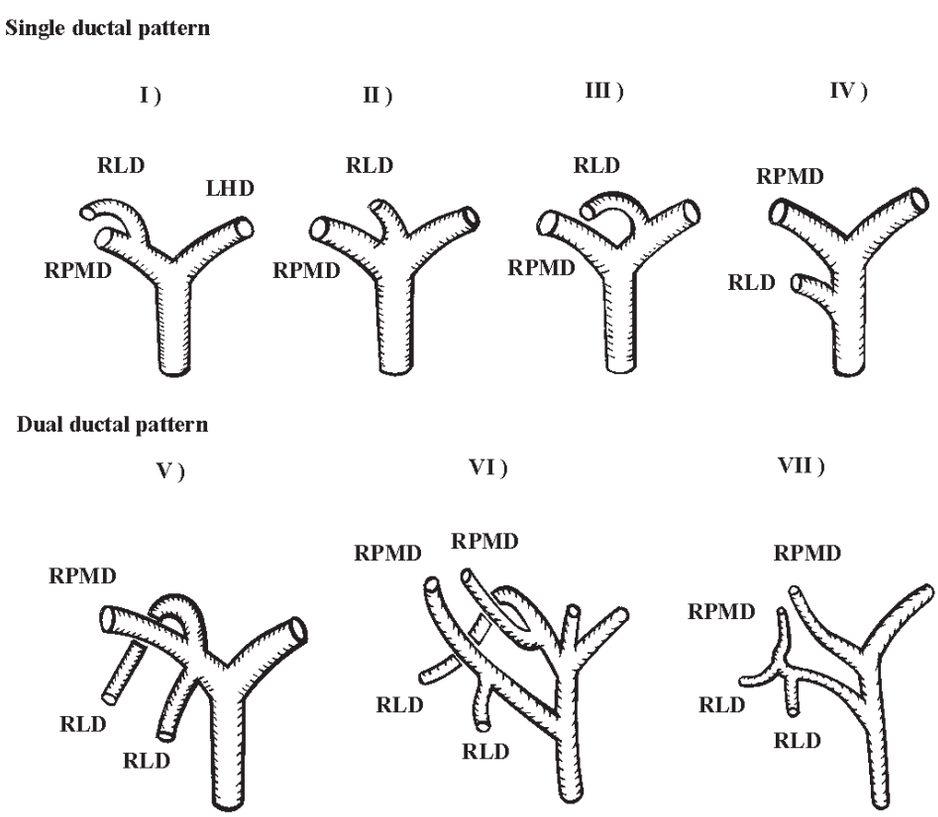

Fig. 4. Anatomical variants of right lateral duct (RLD).
I: 33 cases (63.5%), II: 8 cases (15.4%), Ⅲ: 5 cases (9.6%), Ⅳ : 3 cases (5.8%), V: 1 cases (1.9%), Ⅵ: 1 cases (1.9%), Ⅶ: 1 cases (1.9%)
RPMD: right paramedian duct, RLD: right lateral duct, LHD: left hepatic duct

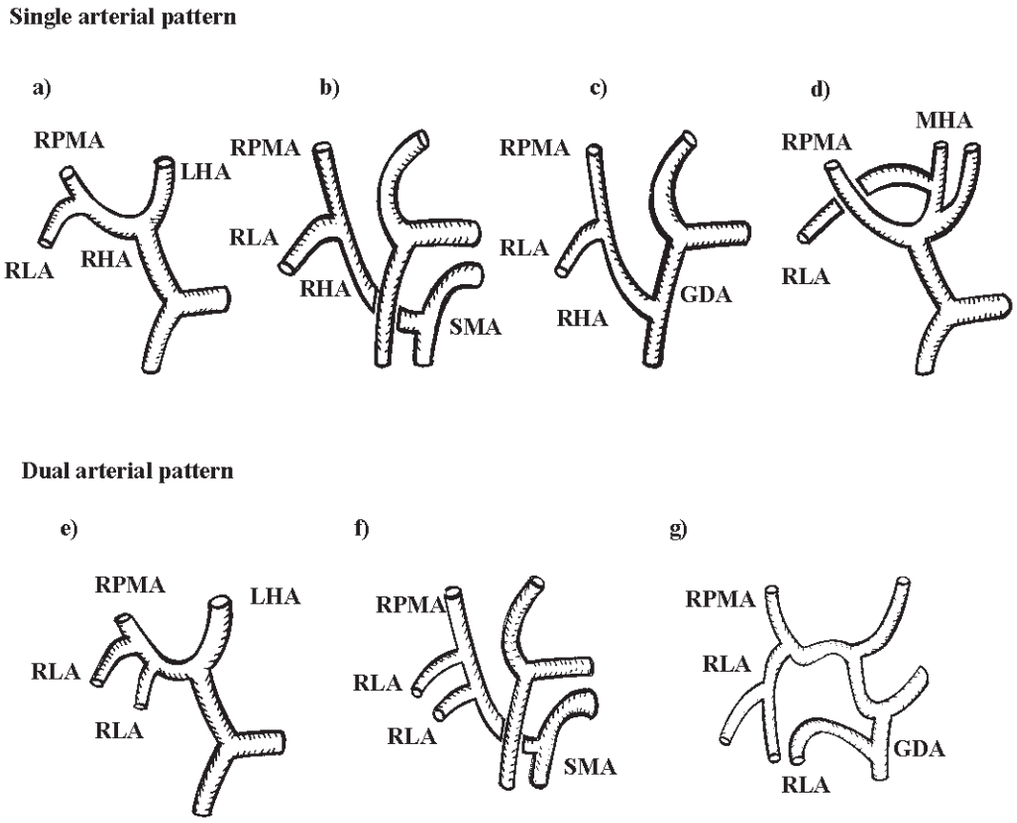

Fig. 5. Anatomical variants of the right lateral artery (RLA).
a) Normal anatomy: 33 cases (63.5%), b) RLA branched from replaced RHA from SMA: 3 cases (5.8%), c) RLA branched from replaced RHA from GDA: 1 case (1.9%), d) RLA branched from MHA; 1 case (1.9%), e) Dual RLAs from RHA: 9 cases (17.3%), f) Dual RLAs from replaced RHA from SMA: 4 cases (7.7%), g) Dual RLA from RHA and from GDA: 1 case (1.9%)
RLA: right lateral artery, RPMA: right paramedian artery, RHA: right hepatic artery, SMA: superior mesenteric artery, MHA: middle hepatic artery, GDA: gastroduodenal artery

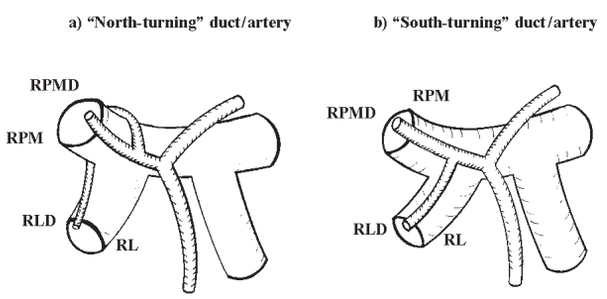

Fig. 6. Running pattern of the light lateral duct/artery.
RPD: right paramedian duct, RLD: right lateral duct, RPM: right paramedian portal vein, RL: right lateral portal vein

vein (RL) and the left portal vein was seen in one patient (type B: 5.8%). In 6 patients, RPM was arising from the left portal vein extrahepatically (type C: 11.5%). Origin of RPM from the intrahepatic part of the left portal vein was seen in another patient (type D: 1.9%). The anomaly in which multiple RPMs originating from the left portal vein (type E) was not seen in any of our patients.

We have classified the branching pattern of RL into 3 types according to its origin from the right portal vein (Fig. 3). In type 1, RL originated from the right portal vein as a single trunk (n= 30, 57.7%). In type 2, although there were two RLs, they originate from the right portal vein by a common ostia (n=10, 19.2%). Origin of two RLs through separate ostia was defined as type 3 (n=12, 23.1%).

Analysis of the biliary system

The pattern of branching of the biliary system in the right lobe is classified into 7 patterns based on the tributary from the right lateral sector (Fig. 4). Forty-nine cases have single right lateral duct (RLD) (I, Ⅱ, Ⅲ and Ⅳ) and 3 have dual RLDs (Ⅴ, Ⅵ and Ⅶ). I is the

normal anatomy in which RLD and the right paramedian duct (RPMD) join to form the right hepatic duct which further joins the left hepatic duct to form the common hepatic duct. Ⅱ is trifurcation of the RLD, the RPMD and the left hepatic duct. In Ⅲ, RLD joins the left hepatic duct (Couinaud's caudal right paramedian duct) [14]. Ⅳ is the joining of the RLD to the common hepatic duct (Couinaud's caudal right lateral duct) [14]. V is dual RLD insertion into RPMD independently (Fig. 8c). In Ⅵ, there are two right hepatic ducts each formed by the joining of separate RPMD and RLD. Ⅶ is multiple RLDs and RPMDs. Incidence of each pattern in our series were I, 33 (63.5%) patients; Ⅱ, 8 (15.4%); Ⅲ, 5 (9.6%); Ⅳ, 3 (5.8%); V, 1 (1.9%); Ⅵ, 1 (1.9%) and Ⅶ, 1 (1.9%) patient.

Analysis of the arteries

The branching pattern of the right lateral artery (RLA) is demonstrated in Fig. 5. The single RLA was observed in 38 patients (73.1%) and dual RLAs in 14 (26.9%). A single RLA arising from the right hepatic artery was seen in 33 patients (Fig. 5a). RLA was originating from a replaced right hepatic artery from the superior mesenteric artery in 3 patients (Fig. 5b) and from the gastroduodenal artery in one patient (Fig 5c). RLA arising from the middle hepatic artery as an accessory artery was seen in another patient (Fig. 5d). Among patients with dual RLAs, in 9, arteries were

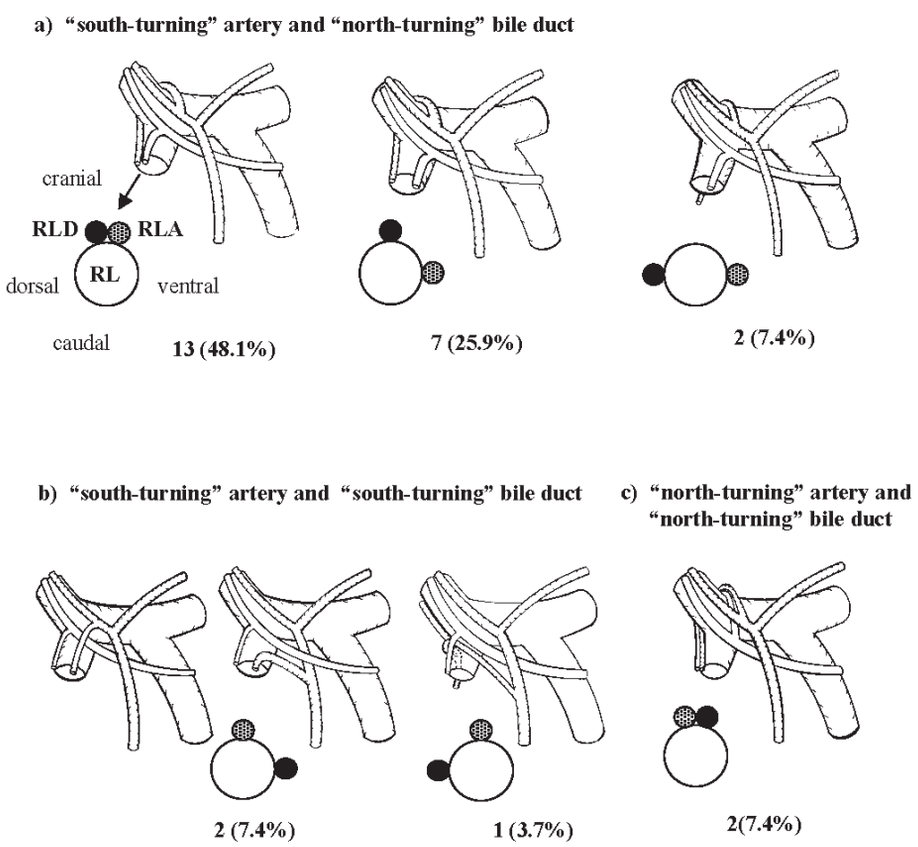

Fig. 7. Running pattern of right lateral portal vein, artery and bile duct for right lateral sector.
Schemes of the sectional plane of the orifice of the RL are presented at the right inferior corner of each figure.

a) "South-turning" artery and "north-turning" bile duct, both artery and bile duct run through the cranial side: 13 cases (48.1%), artery runs through the ventral side with bile duct running through the cranial side: 7 cases (25.9%), and with bile duct running through the dorsal side: 2 cases (7.4%).
b) "South-turning" artery runs through the cranial side with "south-turning" bile duct running through the ventral side: 2 cases (7.4%), and with bile duct running through the dorsal side: 1 cases (3.7%)
c) "North-turning" artery runs through the cranial side with "north-turning" bile duct running through the cranial side: 2 cases (7.4%)

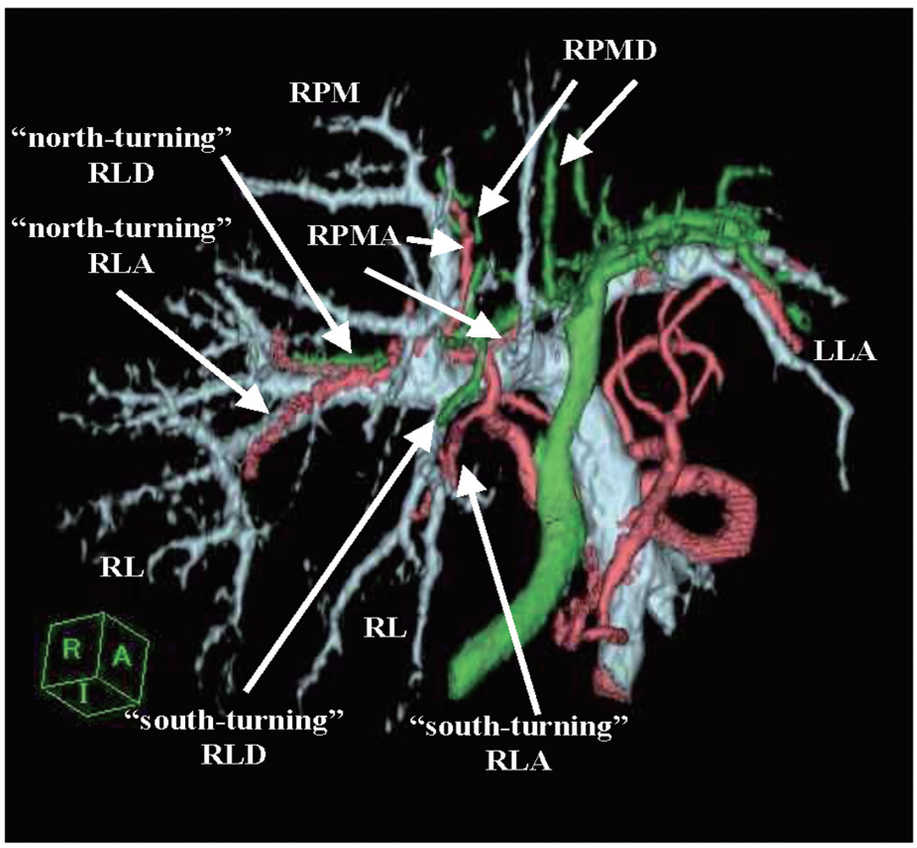

a)

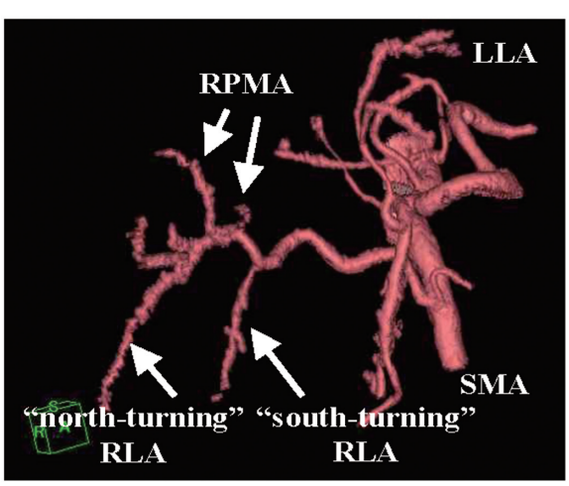

b)

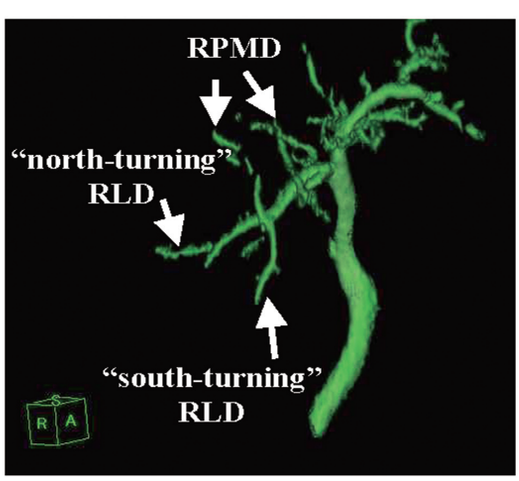

c)

Fig. 8. A case of the dual arteries and the dual bile ducts.

a) RLs were dual, with separate ostia. RLAs and RLDs also were dual. Both RLAs and RLDs showed "north-turning" and "south-turning". The portal vein, bile duct and artery for the right paramedian sector show dual branchings as antero-ventral and antero-dorsal pattern.

b) RLAs were dual. RLAs showed "north-turning" and "south-turning".

c) RLDs were dual. RLDs showed "north-turning" and "south-turning".

originating independently from the right hepatic artery (Fig. 5e). In 4 patients, dual arteries were taking off independently from the replaced right hepatic artery from the superior mesenteric artery (Fig. 5f). Combined supply from a right lateral branch of the right hepatic artery and a branch of the common hepatic artery was also seen in another patient (Fig. 5g).

3D relationship of the artery, the bile duct and the portal vein

3D relationship of the artery and the bile duct to the right lateral sector with reference to the portal vein branches were studied. As showing Fig. 6, we defined the right lateral bile duct/artery which run dorsally and superiorly to RMP as a "north-turning" duct/artery and the bile duct/artery which run ventrally and inferiorly to the right portal vein and RMP as a "south-turning" duct/artery [17]. In 49 patients with single RLD, 44 had the "north-turning" duct (Fig. 6a) and 5 had the "south-turning" duct (Fig. 6b). In 3 patients with multiple RLDs, one had both of the "south-turning" variety and the other two showed a combination of the "north-turning" and the "south-turning" ducts (Fig. 8c). Among 38 cases of single RLA, 8 had "north-turning" artery and 30 had "south-turning" artery. Out of 14 dual RLA cases, in 6, a combination of "north-turning" and "south-turning" (Fig. 8b) arteries were observed. In the remaining 8 cases, all had "south turning" arteries.

3D reconstruction of the single artery-bile duct-portal vein combination for the right lateral sector which was observed in 27 patients is shown in Fig.7. A combination of "south turning" artery and "north turning" duct was the most frequent pattern (22 cases). In all of them, the artery was running cranial or ventral to the bile duct and the portal vein at the sectional plane of origin of RL. The bile duct was sited cranial to the portal vein in 20 cases and dorsal in 2. The "south turning" artery- "south turning" bile duct combination was observed in 3 cases and the "north turning" artery-south turning' duct combination in one. Among patients with these two patterns, 4 had the artery sited dorsally or cranially to the bile duct.

Case presentation (Fig. 8, a, b, c)

RLs were dual, with separate ostia. The dual arteries show "north-turning" and "south-turning", and the dual bile ducts also show "north-turning" and "south-turning". The portal vein, bile duct and artery for the right paramedian sector show dual branchings as antero-ventral and antero-dorsal pattern [19].

DISCUSSION

Reliability of the 3D MD-CT on the anatomical evaluation of the living liver donors has been reported in several articles [12,13,20-23]. The advantages of MD-CT are mainly faster scanning capability, improved temporal resolution, improved spatial resolution and increased effectiveness of the intravascular contrast agent. Sakai et al. [12] reported that, comparing with conventional angiography, 3D CT angiography depicted the extra hepatic arteries and the aberrant arteries successfully and also depicted the intrahepatic segmental arteries with a high detection rate. These results are comparable with the other published literature [13,21]. The portal venous system was also clearly visualized by MD-CT with a high accuracy rate [13]. However, a problem is that 3D reconstruction imaging does not protect against potential misinterpretation during post-processing. As authors did in this study, to increase the reliability of 3D vascular images, it is important to check and pick up the missing branches on sequential 2D images after automatic reconstruction of 3D vascular images by the surgeon himself who is an expert in the anatomy of the hepatic structures.

Contrast enhanced CT was used in this study for the biliary system. Chen et al. [24] reported that CT cholangiography had a good correlation with the images from the endoscopic retrograde cholangiography and the intra-operative cholangiography, and it depicted the tertiary and the quarternary branches of the biliary tree in 99.6% of cases. Accurate depiction of the biliary tree by excretory MR cholangiography using biliary contrast agent Mangafodipir trisodium is reported recently [25,26]. However, Yeh et al. [22] indicated that the biliary enhanced CT cholangiography enabled significantly better biliary tract visualization than the conventional or excretory MR cholangiography either alone or in combination. IV contrast enhanced CT cholangiography is rarely performed in North America partly because of the perceived high risk of the contrast agent [27,28]. However, adverse contrast agent reactions of the biliary enhanced CT can be decreased to 1-3% (similar to the conventional IV contrast enhanced CT) using slow infusion of the contrast agent and premedication with intravenous diphenhydramine [29-32]. Severe side effects which resulted in death were reported to be 0.01% [30,33].

For the understanding of the 3D anatomical relations, integration of the images of the artery, the portal vein and the bile duct will be extremely useful. Dynamic enhanced CT and biliary enhanced CT were

performed at different times in this study because of the possible accelerated adverse effects of the vascular and the biliary contrast media. Each scan was performed with the same focus of view and in post-processing, the 3D position of each image was adjusted accurately on sequential 2D images of axial, sagital and coronal view, focusing the hepatic hilum especially the right portal vein.

Ramification of the first branch of the portal vein has a few anomalies compared with the bile duct and the artery [13]. Nevertheless, as to RL, the single portal vein cases were only 57.7% and others had a common ostia at origin or dual branches without a common right lateral branch. Kyoto team reported that dual portal branches can be reconstructed safely using technical modifications with or without interposed venous graft when the bifurcation is extraparenchymal [18]. However, in institutions with a few experience of LRLT reconstruction of multiple portal branches should be risky and challenging.

Biliary reconstruction is the most challenging part in liver transplantation. Failure to recognize even minor intrahepatic branches crossing the dissection line can result in severe postoperative bile leak and other complications. The incidence of biliary complications in right lobe LRLT is reported to be 10.8-17.5% [18,34] and this is high compared to left-sided liver graft. Nakamura et al. [18] reported that, among 120 right lobe grafts, 43 had dual bile ducts and 4 had triple orifices. Surgical options in multiple ducts can be double reconstructions or reconstruction as a single orifice with or without duct-plasty. They reported that all the biliary variants were successfully reconstructed with an acceptable complication rate (9.3% bile leaks and 8.5% stenosis) in grafts with multiple biliary orifices and concluded that there are no definite contraindications in the biliary anatomy which can preclude a transplantation. However, in right lateral sector LRLT, biliary variantions are more complicated. The duct which runs along the ventral side of RPM is relatively easy to dissect and reconstruct. However, in our series, in 43 cases, RLD showed a 'north turning' pattern-RLD runs along the dorsal side of RPM. The 'north turning' duct is difficult to dissect while procuring the graft because the right paramedian portal vein interferes the dissection. According to Sugawara et al. [35], when the bile duct was sited dorsally to RPM, they pulled the dissected right portal vein and RPM cranially and after that they were able to dissect the bile duct from the surrounding connective tissues. They described that there are no anatomical variations of the bile duct which contraindicate a right lateral sector procuring. Even though, in dual duct cases especially when one duct runs dorsally to the right lateral portal vein and the other ventrally, reconstruction of dual ducts partitioned by the portal vein should be unacceptably difficult. We observed 2 cases with this anomaly.

Because hepatic arterial thrombosis is one of the serious complications after transplantation, arterial anomaly is also a critical consideration in right lateral graft transplantation. The incidence of hepatic artery injury in procurement was significantly higher in grafts with aberrant arterial anomaly and arterial injury was associated with an increased risk of arterial thrombosis [36]. One of our cases had an aberrant RLA arising from the middle hepatic artery. As this anomaly is very rare, accurate anatomical understanding of this artery during the graft procurement is difficult if preoperative imaging of the segmental arterial anatomy is not clearly revealed. This study also revealed that 73.1% of cases had a single RLA and 26.9% had dual RLAs. Among the 38 single artery cases, 8 had 'north turning' right lateral artery. In 6 among the 14 dual artery cases, both or one of the dual arteries was 'north turning'. These 'north-turning' arteries are also difficult to dissect. Further, the arterial branch or branches for the right lateral sector are thinner and shorter than those of the right lobe graft or left-sided graft. Reconstruction of all dual arteries may be difficult in right lateral sector transplant. Whether the presence of multiple arterial branches increases the incidence of hepatic arterial thrombosis remains controversial. Soin et al. [39] recommended that livers with aberrant right hepatic arteries should not to be used because these grafts require multiple arterial reconstructions with a high incidence of postoperative arterial thrombosis. Some institutions are not using left liver grafts with multiple arteries because of the technical difficulties of reconstruction [40,41]. On the other hand, Ikegami et al. [42] recommended to reconstruct only the thickest artery if intraoperative doppler shows pulsatile arterial flow and arterial signal in the corresponding segment of the non-anastomosed arteries. The Tokyo team [43] proposed a simple test on the back table for the selection of single hepatic arterial reconstruction in grafts with multiple arteries. Even though, preoperative precise identification of the hepatic arterial variants by imaging and the accurate assessment of the feasibility are essential components of a successful right lateral graft LRLT.

According to some studies [4,7], in 9-18% of potential donors, the right lateral sector has volumetric advantages compared to the left lobe. However, anomalies of the hepatic vasculature cause further limitations for the feasibility of transplantation. The indica-

tions for the right lateral sector transplantation should have been deliberate at least in institutions which have only a few experiences. In our study, cases having single portal vein, single artery and single bile duct are only 27 among 52 (Fig. 9). Therefore, to increase safe right lateral sector LRLT and to overcome donor shortage, accurate preoperative anatomical evaluation and excellent surgical technique coping with the particular anatomical variant is required. Anatomical understanding based on the 2D images may not be sufficient at operation. The understanding of the 3D vascular and biliary anatomy revealed by this study will contribute to a better definition of the anatomical contraindications for transplantation which may further results in more safe and widely applied right lateral graft LRLT.

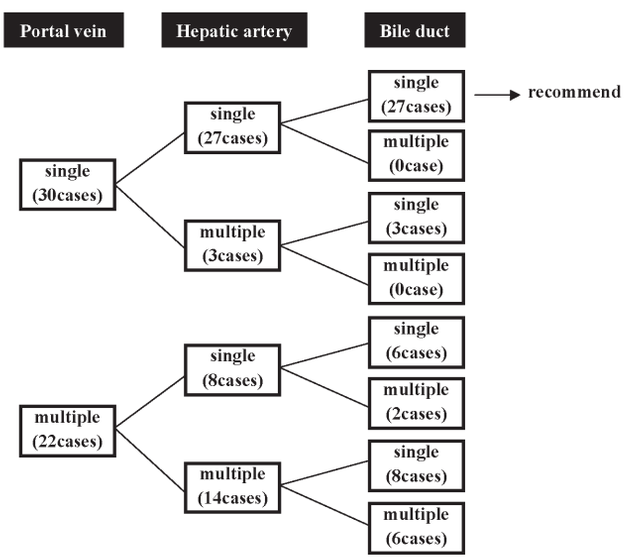

Fig. 9. Anatomical variants of right lateral portal vein, bile duct and artery.

ACKNOWLEDGMENTS: The authors thank Masafumi Uchida M.D., Department of Radiology, Kurume University School of Medicine for providing the MDCT data and for the technical advice.

REFERENCES

1. Tanaka K, Uemoto S, Tokunaga Y, Fujita S, Sano K et al. Surgical techniques and innovations in living related liver transplantation. Ann Surg 1993; 217:82-91.
2. Lo CM, Fan ST, Liu CL, Wei WI, Lo RJ et al. Adult-to-adult living donor liver transplantation using extended right lobe grafts. Ann Surg 1997; 226:261-269.
3. Fan ST, Lo CM, Liu CL, Yong BH, Chan JK et al. Safety of donors in live donor liver transplantation using right lobe grafts. Arch Surg 2000; 135:336-340.
4. Leelaudomlipi S, Sugawara Y, Kaneko J, Matsui Y, Ohkubo T et al. Volumetric analysis of liver Segment in 155 living donors. Liver Transpl 2002; 8:612-614.
5. Kawasaki S, Makuuchi M, Matsunami H, Hashikura Y, Ikegami T et al. Living related liver transplantation in adults. Ann Surg 1998; 227:269-274.
6. Sugawara Y, Makuuchi M, Takayama T, Mizuta K, Kawarasaki H et al. Liver transplantation using a right lateral sector graft from a living donor to her granddaughter. Hepatogastroenterology 2001; 48:261-263.
7. Hwang S, Lee SG, Lee YJ, Park KM, Kim KH et al. Donor selection for procurement of right posterior segment graft in living donor liver transplantation. Liver Transpl 2004; 10:1150-1155.
8. Sugawara Y, Makuuchi M, Takayama T, Imamura H, Kaneko J et al. Right lateral sector graft in adult living-related liver transplantation. Transplantation 2002; 73:111-114.
9. Kim SH, Suh KS, Kim SB, Lee HJ and Lee KU. Adult living donor liver transplantation using right posterior segment. Transpl Int 2003; 16:689-691.
10. Kumashiro Y, Kasahara M, Nomoto K, Kawai M, Sasaki K et al. Living donor liver transplantation for giant hepatic hemangioma with Kasabach-Merritt syndrome with a posterior segment graft. Liver Transpl 2002; 8:721-724.
11. Imamura H, Makuuchi M, Sakamoto Y, Sugawara Y, Kawasaki S et al. Anatomical keys and pitfalls in living donor liver transplantation. J Hepatobiliary Pancreat Surg 2000; 7:380-394.
12. Sakai H, Okuda K, Yasunaga M, Kinoshita H and Aoyagi S. Reliability of hepatic artery configuration in 3D CT angiography compared with conventional angiography-special reference to living-related liver transplant donors. Transpl Int 2005; 18:499-505.
13. Schroeder T, Radtke A, Kuehl H, Debatin JF, Malago M et al. Evaluation of living liver donors with an all-inclusive 3D multi-detector row CT protocol. Radiology 2006; 238:900-910.
14. Couinaud C: Surgical anatomy of the liver revised. Acheve Dimprimer Sur Les Presses, Paris, 1989, 71-72.
15. Zollinger RM. Atlas of surgical operations. 4th ed, Macmillan Publishing Co. Inc., New York, 164-165, 1975.
16. The general rules for the Clinical and Pathological Study of Primary Liver Cancer, November 2000 (The 4th Edition), Liver Cancer Study Group of Japan, 2001, 4-8.
17. Kawarada Y, Das BC and Taoka H. Anatomy of the hepatic hilar area: the plate system.
18. Nakamura T, Tanaka K, Kiuchi T, Kasahara M, Oike F et al. Anatomical variations and surgical strategies in right lobe living donor liver transplantation: lessons from 120 cases. Transplantation 2002; 73:1896-1903.
19. Hashimoto T, Sugawara Y, Kishi Y, Akamatsu N, Matsui Y et al. Reconstruction of the middle hepatic vein tributary in a right lateral sector graft. Liver transplantation 2005; 11:309-313.
20. Chen YF, Lee TY, Chen CL, Huang TL, Chen YS et al. Three-dimensional helical computed tomographic cholangiography: application to living related hepatic transplantation. Clin Transplant 1997; 11:209-213.

21. Lee SS, Kim TK, Byun JH, Ha HK, Kim PN et al. Hepatic arteries in potential donors for living related liver transplantation: evaluation with multi-detector row CT angiography. Radiology 2003; 227:391-399.
22. Yeh BM, Breiman RS, Taouli B, Qayyum A, Roberts JP et al. Biliary tract depiction in living potential liver donors: comparison of conventional MR, mangafodipir trisodium-enhanced excretory MR, and multi-detector row CT cholangiography-initial experience. Radiology 2004; 230:645-651.
23. Hirao K, Miyazaki A, Fujimoto T, Isomoto I and Hayashi K. Evaluation of aberrant bile ducts before laparoscopic cholecystectomy: helical CT cholangiography versus MR cholangiography. Am J Roentgenol 2000; 175:713-720.
24. Chen YF, Lee TY, Chen CL, Huang TL, Chen YS et al. Three-dimensional helical computed tomographic cholangiography: application to living related hepatic transplantation. Clin Transplant 1997; 11:209-213.
25. Lee VS, Krinsky GA, Nazzaro CA, Chang JS, Babb JS et al. Defining intrahepatic biliary anatomy in living liver transplant donor candidates at mangafodipir trisodium-ehanced MR cholangiography versus conventional T2-weighted MR cholangiography. Radiology 2004; 233:659-666.
26. Kapoor V, Peterson MS, Baron RL, Patel S, Eghtesad B et al. Intrahepatic biliary anatomy of living adult liver donors: Correlation of Magafordipir trisodium- enhanced MR cholangiography and intraoperative cholangiography. AJR Am J Roenterol 2002; 179:1281-1286.
27. Ott D and Gelfand D. Complications of gastrointestinal radiologic procedures. Ⅱ. Complications related to biliary tract studies. Gastrointest Radiol 1981; 6:47-56.
28. Rholl K, Smathers R, Mclennan B and Lee J. Intravenous cholangiography in the CT era. Gastrointest Radiol 1985; 10:69-74.
29. Van Beers BE, Lacrosse M, Trigax J, Cannire LD, De Ronde T et al. Noninvasive imaging of the biliary tree before or after laparoscopic cholecystectomy: use of three dimensional spiral CT cholangiography. AJR Am J Roenterol 1994; 162:1331-1335.
30. Nilsson U. Adverse reaction to iotroxate at intravenous cholangiography: a prospective clinical investigation and review of the literature. Acta Radiol 1987; 28:571-575.
31. Maglinte D and Dorenbusch M. Intravenous infusion cholangiography: an assessment of its role relevant to laparoscopic cholecystectomy. Radiol Diagn 1993; 34:91-96.
32. Sacharias N. Safety of Biliscopin (letter). Australas Radiol 1995; 39:101.
33. Fleischmann D, Ringl H, Schofl R, Potzi R, Kontrus M et al. Three-dimensional spinal CT cholangiography in patients with suspected obstructive biliary disease: comparison with endoscopic retrograde cholangiography. Radiology 1996; 198:861-868.
34. Marcos A, Ham JM, Fisher RA, Olzinski AT and Posner MP. Surgical management of anatomical variations of the right lobe in living donor liver transplantation. Annals of Surgery 2000; 231:824-831.
35. Sugawara Y and Makuuchi M. Right lateral sector graft as a feasible option for partial liver transplantation. Liver Transpl 2004; 10:1156-1157.
36. Nijkamp DM, Slooff MJ, van der Hilst CS, Ijtsma AJ, de Jong KP et al. Surgical injuries of postmortem donor livers: incidence and impact on outcome after adult liver transplantation. Liver Transpl 2006; 12:1365-1370.
37. Ikegami T, Kawasaki S, Matsunami H, Hashikura Y, Nakazawa Y et al. Should all hepatic arterial branches be reconstructed in living-related liver transplantation? 1996; 119:431-436.
38. Tanaka K, Uemoto S, Tokunaga Y, Fujita S, Sano K et al. Surgical techniques and innovations in living-related liver transplantation. Ann Surg 1993; 217:82-91.
39. Soin AS, Friend PJ, Rasmussen A, Saxena R, Tokat Y et al. Donor arterial variations in liver transplantation: management and outcome of 527 consecutive grafts. Br J Surg 1996; 83:637-641
40. Kostelic JK, Piper JB, Leef JA, Lu CT, Rosenblum JD et al. Angiographic selection criteria for living related liver transplantation. AJR Am J Roentgenol 1996; 166:1103-1108.
41. Broelsch CE, Whitington PF, Emond JC, Heffron TG, Thistlethwaite JR et al. Liver transplantation in children from living related donors. Surgical techniques and results. Ann Surg 1991; 214:428-437.
42. Ikegami T, Hashikura Y, Nakazawa Y, Urata K, Mita A et al. Risk factors contributing to hepatic artery thrombosis following living-donor liver transplantation. J Hepatoboliary Pancret Surg 2006; 13:105-109.
43. Kubota K, Makuuchi M, Takayama T, Harihara Y, Hasegawa K et al. Simple test on the back table for justifying single hepatic-arterial reconstruction in living related liver transplantation. Transplantation 2000; 70:696-697.

Original Contribution

Kurume Medical Journal, 55, 55-62, 2008

Evaluation of a Real-Time PCR Assay for the Diagnosis of *Pneumocystis* pneumonia

KOHJU ETOH

Department of Medicine, Kurume University School of Medicine, Kurume 830-0011, Japan

Received 3 March 2008, accepted 16 February 2009

Edited by KOICHI KUWANO

Summary: The aim of this study was to evaluate of the quantification of *Pneumocystis jiroveci* using a real-time PCR assay. We tried to verify whether quantification was really effective in differentiating between carriage and *Pneumocystis* pneumonia (PCP) using real-time PCR with or without sample species normalization for classifying each sample species (sputum, bronchoalveolar lavage : bronchoalveolar lavage (BAL), and total samples).

Twenty-two positive samples previously examined by conventional qualitative PCR were subjected to real-time PCR. Of these 22 lower respiratory tract specimens, 10 were BAL samples and 12 were (induced) sputum samples. According to our clinical diagnostic criteria, 17 were PCP and 5 were non-PCP. In the 12 sputum samples the concentrations of *Pneumocystis*-specific DNA detected in the non-PCP patients did not differ significantly from those in the PCP patients. The data were normalized using glyceraldehyde-3-phosphate dehydrogenase (GAPDH) as the housekeeping gene to exclude differences due to the number of human cells in collected samples. After normalization, the *Pneumocystis*-specific DNA/GAPDH-DNA ratio in the non-PCP patients was higher than that in the PCP patients. In the BAL samples (10 samples), the mean concentration of *Pneumocystis*-specific DNA detected in the PCP patients was 9.6 times higher than that in the non-PCP patients (P=0.058), and after normalization, the *Pneumocystis*-specific DNA/GAPDH-DNA ratio in the PCP patients did not differ significantly (P=0.19) from that in the non-PCP patients. Although the present study indicated that normalization using GAPDH might be not helpful but BAL specimens are recommended over sputum specimens for the diagnosis of *Pneumocystis* Pneumonia by quantification with real-time PCR.

Key words PCP, realtime PCR, normalization, GAPDH, BAL

INTRODUCTION

Pneumocystis jiroveci, formerly known as *Pneumocystis carinii* f. sp. *Hominis*, is an important cause of morbidity and mortality, causing *Pneumocystis* pneumonia (PCP) in patients whose immune systems have been compromised due to disease and/or immunosuppressive treatments. The standard method for the diagnosis of PCP is microscopic examination of stained (Giemsa and Grocott techniques) invasive lower respiratory tract specimens from bronchoalveolar lavage (BAL), lung biopsy, aspirates or induced sputum specimens. This method has relatively low sensitivity but high specificity [3,13,17,29,33]. Molecular detection systems such as PCR techniques have the potential to provide a higher degree of sensitivity than microscopic examinations [1-4,7,8,12,16,17,20-23,25,28,29-32]. Due to the high sensitivity of molecular methods, *Pneumocystis jiroveci* DNA has been detected in respiratory samples from patients without PCP, probably representing either colonization or subclinical infection, at a rate of 2.2-40% [7,9,15-22,24,25,27,28].

It is thought that real-time PCR, as recently described [5,14], might be useful in distinguishing between colonization and clinical disease. This sugges-

Corresponding author: KOHJU ETOH, Department of Medicine, Kurume University School of Medicine, Kurume 830-0011, Japan. Tel: 0942-31-7560 Fax: 0942-31-7560 Fax: 0942-31-7703

Abbreviations: BAL, bronchoalveolar lavage; PCP, *Pneumocystis* pneumonia.

tion is based on the hypothesis that PCP patients should have a higher organism burden than colonized or subclinically infected patients, and that this would be reflected by a higher amount of *Pneumocystis jiroveci* DNA present in the extracted specimens from PCP patients. However, sample quality and quantity can vary significantly from person to person, and the quality of the sputum and the rate of retrieval of BAL fluid can differ each time a sample is collected.

Therefore, we postulated that normalization using GAPDH, a human house-keeping gene, might overcome these limitations, and evaluated the quantification of *Pneumocystis jiroveci* using a real-time PCR with sample species normalization.

MATERIALS AND METHODS

Subjects

Samples for this study came from all patients evaluated by the Department of Medicine, Division of Respirology, Neurology, and Rheumatology, and other 2 divisions (Gastroenterology, Nephrology) and other 2 Departments (Pediatrics, Acute medicine), Kurume University School of Medicine and other hospital (Kurume University Medical Center) between May 2000 and August 2004 who presented with clinical symptoms of pulmonary infection associated with immunosuppression, thus justifying a search for Pneumocystis in BAL and induced sputum specimens.

Thirty-two positive samples, previously examined by conventional qualitative PCR, were utilized for real-time PCR. In 22 of these 32 samples, we were able to verify the data. Ten samples were excluded because the PCR would not be able to evaluate. Therefore 22 lower respiratory tract specimens were collected from 22 patients with immunosuppression due to various diseases and/or immunosuppressive treatments: 10 BAL samples and 12 induced sputum samples. The ten BAL samples comprised 5 specimens retrieved by washing with only 20 ml of 0.9% NaCl (BAL-20) due to the patient's severe respiratory status. Four were retrieved by washing with 100 ml of 0.9% NaCl (BAL-100) and 1 was retrieved by washing with only 10ml of 0.9% NaCl (BAL-10) due to the patient's age (only 2 months).

Preparation of DNA specimens

Patient sputum samples were incubated with an equal volume of Sputazyme (semialkaline proteinase, 200 mg/vial; Na_2HPO_4, 16.25 mg/ml; KH_2PO_4, 2.88 mg/ml [pH 7.2]; Kyokuto Pharmaceutical Co., Ltd. Tokyo, Japan) at 37°C for 10 min. The samples were centrifuged at 1,600 × g for 15 min. The pellets were resuspended in 0.5 ml of TE buffer (10 mM Tris-Cl, 1 mM EDTA [pH 7.5]) and then spun for 10 sec at 13,000 × g. This procedure was repeated twice, and the final pellet was resuspended in 200 μl of InstaGene DNA Purification Matrix (Bio-Rad Laboratories, Inc.). The mixture was incubated for 15 min at 56°C, vortexed for 10 sec, incubated for 8 min at 100°C, vortexed for 10 sec and then spun at 13,000 rpm for 2 min. The BAL fluid samples were centrifuged at 1,600 × g for 10 min. The pellets were resuspended in 1 ml of phosphate-buffered saline and then incubated with an equal volume of Sputazyme. These samples were treated in the same manner as the sputum samples. We used 2 μl of this supernatant as the DNA sample.

Conventional PCR

PCR was performed according to Honda et al. [11]. For the detection of Pneumocystis-specific DNA, the primers PAZ102-E (5'-GATGGCTGTTTC-CAAGCCCA-3') and PAZ102-H (5'-GTGTACGTT-GCAAAGTACTC-3'), derived from the mitochondrial large subunit rRNA (*mtLSUrRNA*), and which amplified a 346 bp sequence, were used as reported previously [31].

Real-time PCR with the LightCycler

PCR conditions: The real time PCR assay involves LightCycler technology, which combines rapid thermocycling with on-line fluorescence detection of the PCR products. The reactions were performed in a volume of 20 μl of a mixture containing 0.01 mM of each primer and 2 μl of LightCycler FastStart DNA Master SYBR Green I (Roche Diagnostics GmbH Roche Applied Science Nonnenwald 282372 Penzberg Germany) containing FastStart Taq DNA polymerase, reaction buffer, dNTP mix (with dUTP instead of dTTP), SYBR Green I dye, and 10 mM $MgCl_2$. The final concentration of $MgCl_2$ was adjusted to 3 mM. The samples were placed into LightCycler capillaries (20μl) (Roche Diagnostics GmbH Roche Applied Science Nonnenwald 282372 Penzberg Germany), capped, centrifuged for a few seconds in a micro-centrifuge using appropriate adapters, and placed into the LightCycler rotor. An initial preheating step of 10 min at 95°C was used to activate the DNA polymerase, deactivate UNG, and melt double-stranded DNA. Next, a touch-down procedure followed, consisting of 15 sec at 95°C, annealing for 10 sec at temperatures decreasing from 65 to 60°C during the first 11 cycles (with 0.5°C decremental steps in each cycle), and ex-

tension at 72°C for 15 sec, and acquisition of the fluorescent signal from the samples at 80°C for 2 sec to increase the specificity of PCP specific DNA. Acquisition of the fluorescent signal from the samples was performed at 82°C for 2 sec to increase the specificity of GAPDH DNA. The transition rate of temperature was set at 20°C/sec for denaturation to annealing and from annealing to extension and extension to denaturation. A total of 45 cycles were performed. The PCR products were subjected to analysis by electrophoresis on a 2% agarose gel to confirm the efficiency of the melting curve analysis.

Standards and external controls: To obtain standards for real-time PCR, *P. jiroveci*-positive BAL samples (by Grocott smear) were used. The extracted DNA (described above in *Preparation of DNA specimens*) was used for amplification of the major surface glycoprotein (MSG) gene of *Pneumocystis* [14]. A PCR method previously described [11] was modified for the real-time assay. The commercially synthesized primers (Operon Biotechnologies, Inc. Tokyo, Japan) JKK14/15 (5'-GAA TGC AAA TCY TTA CAG ACA ACA G-3') and JKK17 (5'-AAA TCA TGA ACG AAA TAA CCA TTG C-3') amplified a 250-bp segment of the multicopy MSG gene family [14]. The amplified products were subjected to electrophoresis in agarose gels, and bands were visualized with UV light following ethidium bromide staining.

To detect amplicons (*Pneumocystis* DNA) in agarose gels (TBE buffer), trimmed gel slices and the chopped pieces were used for DNA extraction with Quantum Prep Freeze'N Squeeze DNA Gel Extraction Spin Columns (Bio-Rad Laboratories, Inc.) according to the manufacturer's recommendations. The extracted DNA was amplified using JKK14/15 and JKK17 primers, and the amplicon was confirmed as a 250 bp sequence by electrophoresis in agarose gels (described above). The GAPDH samples were confirmed in the same manner as the respective *Pneumocystis* samples. The commercially synthesized primers (Operon Biotechnologies, Inc. Tokyo, Japan) GAPDH-sense (5'-CTT CAC CAC CAT GGA GAA GGC-3') and JKK17 (5'-GGC ATG GAC TGT GGT CAT GAG-3') amplified a 260-bp segment. The concentration was determined using a ND-1000 Spectrophotometer (NanoDrop Technologies) and the *A*260 and *A*280 optical density measurements. Sample species normalization was calculated as the ratio of *Pneumocystis*-specific DNA/GAPDH-DNA. GAPDH was used as a housekeeping gene.

Data analysis

Diagnosis of PCP based on microscopic examination of stained samples is difficult because of the low sensitivity for detection of *Pneumocystis* cells. The criteria that we used for confirming ongoing pneumocystosis were clinical findings of PCP with characteristic X-ray findings (new bilateral diffuse interstitial infiltrates), dyspnoea with/without arterial hypoxaemia (partial pressure of arterial oxygen <70 mmHg) as well as response to anti-*Pneumocystis* treatment but resistance to other antibiotics or response to both anti-*Pneumocystis* treatment and other antibiotics. Based on these diagnostic criteria, the quantities and normalized quantities were evaluated. Statistical assessment of these characteristics was performed using the Fisher's test and G test ($P<0.05$ was considered significant). Statistical assessment of differences of the mean of *Pneumocystis* DNA concentration [$\times$1/10fg/μl] from PCP or non-PCP cases was performed by the unpaired Student's t-test ($P<0.05$ was considered significant).

RESULTS AND DISCUSSION

According to our diagnostic criteria, of the 22 patients profiled, 17 had developed PCP. In the remaining 5, the diagnosis of PCP was not confirmed.

Quantitative PCR

Total samples (sputum and BAL)

In the 22 samples, the mean concentrations ($\times$1/10fg/μl) of *Pneumocystis*-specific DNA detected in the non-PCP patients and PCP patients were 3.85×10^7 and 3.51×10^6, respectively (Fig. 1-a). The mean concentration of the non-PCP patients was significantly higher than that of the PCP patients ($p<0.05$). The mean concentrations ($\times$1/10fg/μl) of GAPDH-DNA detected in the non-PCP patients was significantly higher than that in the PCP patients ($P<0.05$). The mean concentrations of GAPDH-DNA in the non-PCP patients and PCP patients were 8.64×10^7 and 1.23×10^7, respectively (Fig. 1-b). After normalization, the ratio of Pneumocystis-specific DNA/GAPDH-DNA in the non-PCP patients did not differ significantly ($p=0.41$) from that of the PCP patients (Fig. 1-c; the mean ratio of the non-PCP patients was 0.26 while the mean ratio of the PCP patients was 0.23). Normalization was considered necessary because the qualities and quantities of the various samples were variable, and the quality of the sputum and the rate of retrieval of BAL differed from

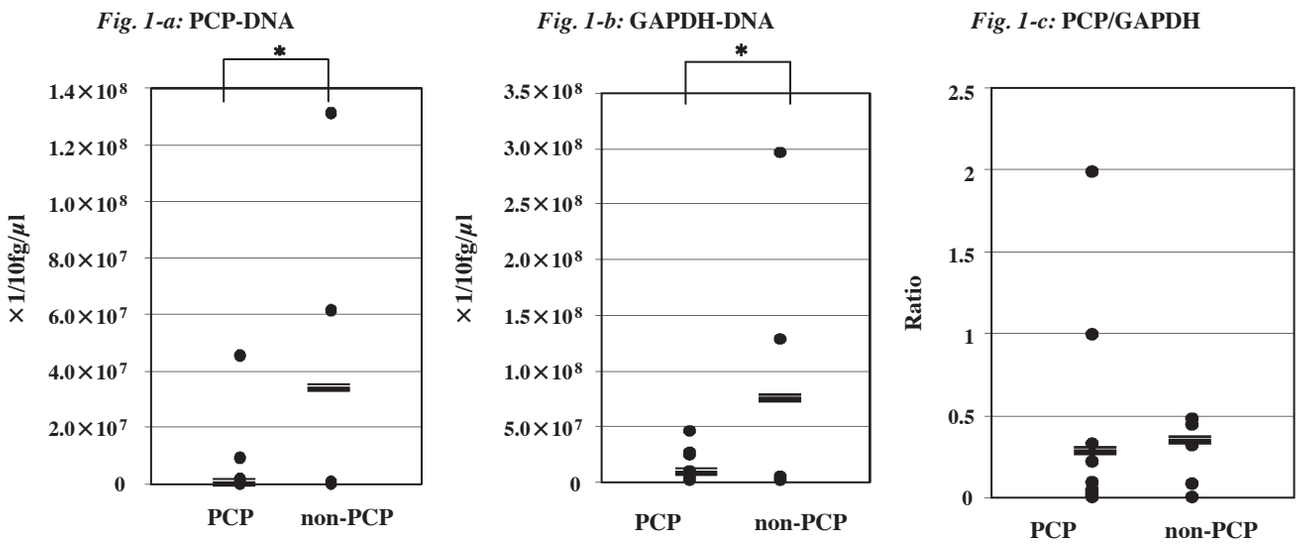

Fig. 1. Quantity of DNA in both the sputum and BAL samples by clinicalcategory.
Fig. 1-a: PCP-DNA concentrations in the PCP cases [n=17] and the non-PCP cases [n=5]. The mean concentrations (×1/10fg/μl): The mean PCP-DNA concentration in the PCP positive patients was 3.51×10^6; the mean PCP-DNA concentration in the non-PCP patients was 3.85×10^7; $P<0.05$.
Fig. 1-b: GAPDH-DNA concentrations in the PCP cases [n=17] and the non-PCP cases [n=5]. The mean concentrations (×1/10fg/μl): The mean GAPDH-DNA concentration in the PCP positive patients was 1.23×10^7; the mean GAPDH-DNA concentration in the non-PCP patients was 8.64×10^7; $P<0.05$.
Fig. 1-c: PCP/GAPDH ratio in the PCP cases [n=17] and the non-PCP cases [n=5]. The mean ratios: The mean PCP/GAPDH ratio in the PCP positive patients was 0.23; the mean PCP/GAPDH ratio in the non-PCP patients was 0.26; P=0.41. Symbols: =, mean; *, $P<0.05$.

patient to patient. Normalization was performed using the ratio of *Pneumocystis*-specific DNA/GAPDH-DNA. GAPDH is a housekeeping gene that is stably expressed with little variation in human cells. Therefore, we used GAPDH for normalization in order to calculate the amount of PCP DNA relative to the number of the cells calculated. However, our results showed no significant difference between PCP and non-PCP patients after normalization. In microscopic examinations of stained sputum, the smear positive rate with instruction was higher than that without instruction (according to the classification of Miller and Jones)[10], and according to the classification of Geckler et al. [6], microscopic screening along with the rejection of unsatisfactory specimens can minimize the unreliability of sputum culture. We therefore considered that the evaluation of sputum quality and preparation might be required for the quantification of PCR studies. In the BAL samples, the amount that was retrieved by washing with 100 ml of 0.9% NaCl (BAL-100) was variable in each sample.

From previous reports on qualitative PCR, the sensitivity of BAL samples was higher than that of sputum samples [4,23,29], or was nearly equal [26,30].

In a qualitative PCR study Larsen et al. [14] reported that sputum samples were PCR positive but the differences between the PCP and non-PCP patients in the quantitative PCR results from the induced sputa did not reach the level of significance. Therefore we analyzed our data after classifying the sample specimens (sputum and BAL).

Sputum samples (Fig. 2)

In the sputum samples (12 samples), the concentration of Pneumocystis-specific DNA detected in the non-PCP patients (n=3) did not significantly differ from that of the PCP patients (n=9). The mean concentrations (×1/10fg/μl) were 6.41×10^7 and 6.24×10^6 in the non-PCP and PCP patients, respectively (Fig. 2-a). The concentrations of GAPDH-DNA detected in the non-PCP patients were higher than those in the PCP patients ($P<0.01$). The mean concentrations (×1/10fg/μl) were 1.42×10^8 and 1.35×10^7 in the non-PCP and PCP patients, respectively (Fig. 2-b). After normalization, the ratio of *Pneumocystis*-specific DNA/GAPDH-DNA in the non-PCP patients was significantly higher ($P<0.05$) than that in the PCP patients. The mean ratios were 0.41 and 0.19 in the non-PCP and PCP patients, respectively (Fig. 2-c).

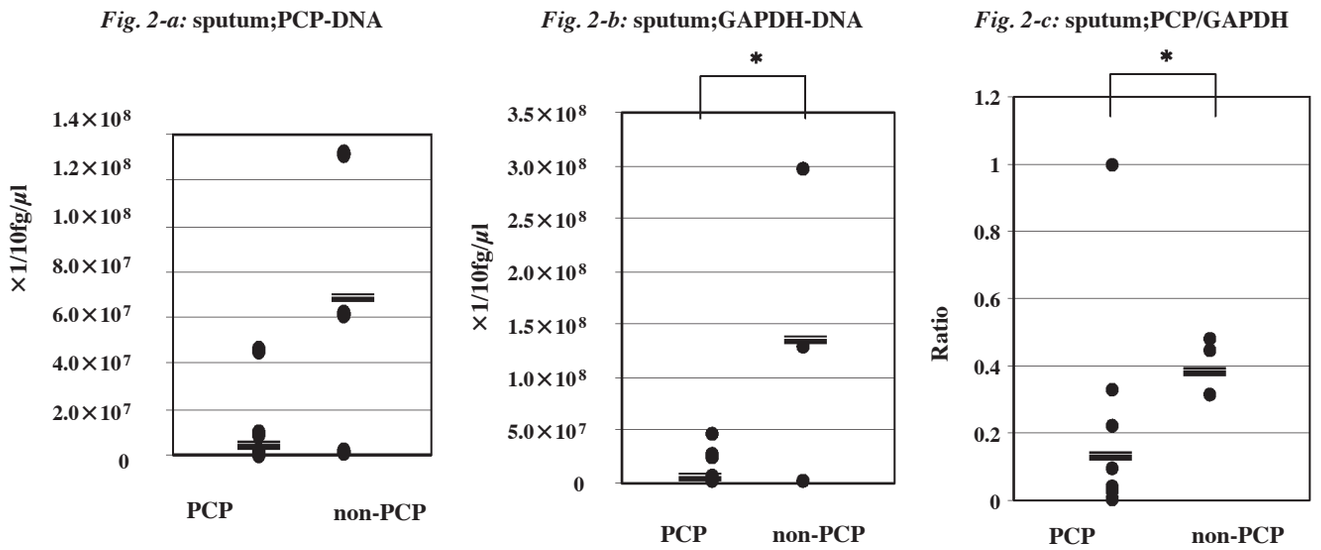

Fig. 2. Quantity of DNA in the sputum samples by clinical category.

Fig. 2-a: PCP-DNA concentrations in the PCP cases [n=9] and the non-PCP cases [n=3]. The mean concentrations (×1/10fg/μl): The mean PCP-DNA concentration in the PCPpositive patients was 6.24×10^{6}; the mean PCP-DNA concentration in the non-PCP patients was 6.41×10^{7}; P=0.13.

Fig. 2-b: GAPDH-DNA concentrations in the PCP cases [n=9] and the non-PCP cases [n=3]. The mean concentrations (×1/10fg/μl): The mean GAPDH-DNA concentration in the PCP positive patients was 1.35×10^{7}; the mean GAPDH-DNA concentration in the non-PCP patients was 1.42×10^{8}; P<0.01.

Fig. 2-c: PCP/GAPDH ratios in the PCP cases [n=9] and the non-PCP cases [n=3]. The mean ratios: The mean PCP/GAPDH ratio in the PCP positive patients was 0.19; the mean PCP/GAPDH ratio in the non-PCP patients was 0.41; P<0.05. Symbols: =, mean; *, P<0.05.

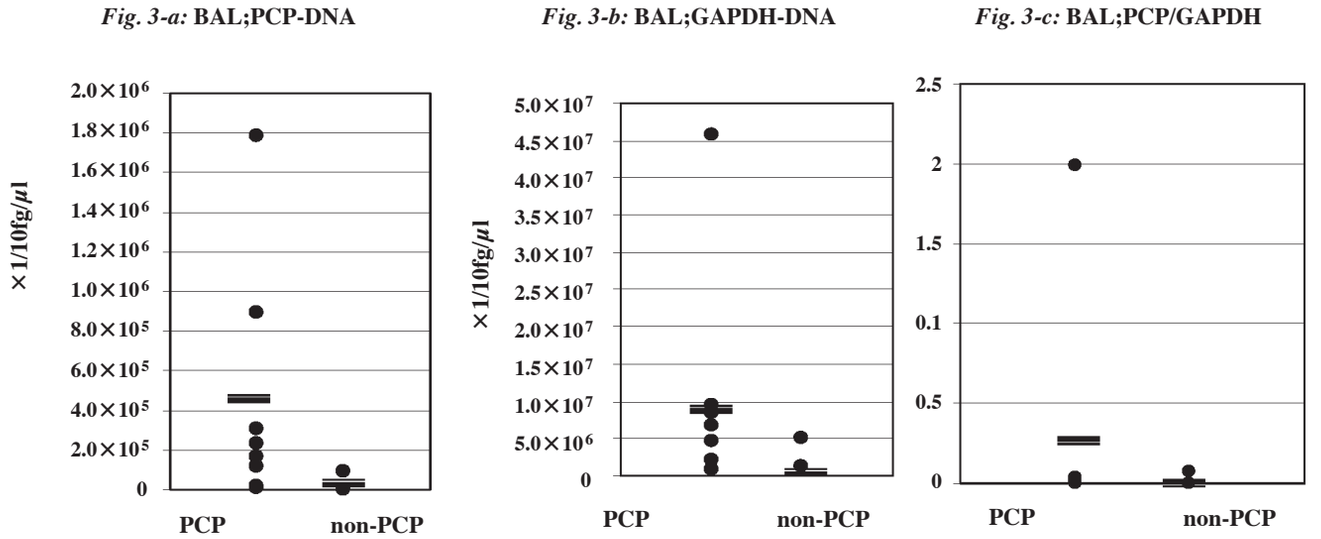

Fig. 3. Quantity of DNA in the BAL samples by clinical category.

Fig. 3-a: PCP-DNA concentrations in the PCP cases [n=8] and non-PCP cases [n=2]. The mean concentrations (×1/10fg/μl): The mean PCP-DNA concentration in the PCP positive patients was 4.40×10^{5}; the mean PCP-DNA concentration in the non-PCP patients was 4.59×10^{4}; P=0.058.

Fig. 3-b: GAPDH-DNA concentrations in the PCP cases [n=8] and the non-PCP cases [n=2]. The mean concentrations (×1/10fg/μl): The mean GAPDH-DNA concentration in the PCP positive patients was1.08×10^{7}; the mean GAPDH-DNA concentration in the non-PCP patients was 3.14×10^{6}; P=0.099.

Fig. 3-c: PCP/GAPDH ratios in the PCP cases [n=8] and the non-PCP cases [n=2]. The mean ratios: The mean PCP/GAPDH ratio in the PCP positive patients was 0.27; the mean PCP/GAPDH ratio in the non-PCP patients was 0.039; P=0.19. Symbols: =, mean; *, P<0.05.

BAL samples (Fig. 3)

In the BAL samples (10 samples), the mean concentration of *Pneumocystis*-specific DNA detected in the PCP patients was 9.6 times higher than that in the non-PCP patients (P=0.058). The mean concentrations ($\times$1/10fg/μl) were 4.40×10^5 and 4.59×10^4 in the PCP and non-PCP patients, respectively (Fig. 3-a). The mean concentrations ($\times$1/10fg/μl) of GAPDH-DNA detected in the PCP and non-PCP patients were 1.08×10^7 and 3.14×10^6, respectively (Fig. 3-b). After normalization, the ratio of *Pneumocystis*-specific DNA/GAPDH-DNA in the PCP patients did not differ significantly from that in the non-PCP patients (Fig. 3-c). In the PCP patients, lung tissue is often injured and a large number of human cells are obtained from the BAL samples. GAPDH quantity might reflect the amounts of human cells in samples. The samples from inflammatory lesion might have more inflammatory cells than those from non-inflammatory did. Therefore, the ratios of *Pneumocystis*-specific DNA/GAPDH-DNA may not reflect the concentration of PCP.

Although we thought that sample normalization with a housekeeping gene might be effective in helping to determine a cut-off value, it turned out to yield a meaningless result. This might have been due to the underlying primary disease. In particular, results might differ between HIV-positive and -negative cases. Such a difference has been found in previous studies, which have indicated the difficulty of confirming a PCP diagnosis in non-HIV-infected cases due to the lack of sensitivity of PCR methods (20-25%), even in BAL specimens [5,23,25,32]. The PCR positive rate for PCP in the HIV positive patients was higher than that in the HIV negative patients (6/8:75%>2/8:25%) [7].

In our cases, no HIV positive patient was PCP

TABLE 1.
Comparison of each parameters in Pneumocystis pneumonia (PCP) patinents

case	sample species	primary disease	age (year)	gender	WBC (/μL) (LYM%)	lymphcyte /μL	CRP (mg/dL)	beta-D-glucan (pg/mL) (<11)	Quantitave PCR (PCP)	Quantitave PCR (GAPDH)	(PCP/GAPDH)
1	BAL-20	SLE	37	F	3800(6)	228	6.3	86.9	1.78×10^6	8.92×10^5	2.0
2	BAL-10	SCID	2 months	F	1900(36)	684	0.3	3.5	1.15×10^5	6.70×10^6	<0.1
3	BAL-100	RPGN due to MPA	71	F	10500(15.5)	1627.5	5.9	181.1	3.03×10^5	8.52×10^6	<0.1
4	Sputum	MG/Thymoma (invasive type)	71	F	6700(6.0)	402	9.1	563.1	8.79×10^6	2.67×10^7	0.3
5	Sputum	Lung cancer	74	M	6200(2.0)	124	6.6	204.4	4.43×10^4	1.77×10^6	<0.1
6	Sputum	Lung cancer	69	F	6900(2.0)	138	28.1	395.7	2.79×10^5	6.85×10^6	<0.1
7	Sputum	Lung cancer	71	M	5300(16.1)	853.3	13.9	3.5	1.15×10^6	5.22×10^6	0.2
8	Sputum	Multiple Myeloma	62	F	700(34)	238	24.0	2.9	1.71×10^2	3.89×10^6	<0.1
9	BAL-100	MPA	67	F	10400(2.5)	260	4.3	214.5	1.69×10^5	4.64×10^6	<0.1
10	BAL-20	RPGN due to mPA/Psoriasis	60	M	6800(15)	1020	6.1	104.2	8.95×10^5	4.58×10^7	<0.1
11	BAL-20	CRF/cryoglobulinemia/LC-C	72	F	8200(/)	/	2.9	117.7	2.31×10^5	8.64×10^6	<0.1
12	Sputum	Lung cancer,SVC syndrome	74	M	8600(3)	258	1.6	11.5	4.52×10^7	4.55×10^7	1.0
13	BAL-20	Lung cancer	69	M	8500(1)	85	30.6	13.1	1.46×10^4	9.47×10^6	<0.1
14	Sputum	PN/pulmonary tuberculosis/ Post MVR	59	M	5900(2)	118	6.4	100.8	3.77×10^2	2.44×10^6	<0.1
15	Sputum	Systemic Scrlosis	64	F	6400(/)	/	3.9	165.2	1.66×10^5	2.34×10^7	<0.1
16	Sputum	Malignant Lymphoma relapse	82	M	1900(29.5)	560.5	5.8	36	5.68×10^5	6.13×10^6	<0.1
17	BAL-20	SLE+chronic thyroiditis	48	M	10000(17)	1700	6.7	134.7	6.46×10^3	2.03×10^6	<0.1

* BAL-100, BAL fluid specimen after washing with 100 ml 0.9% NaCl; BAL-20, BAL fluid specimen after washing with 20 ml 0.9% NaCl; BAL-10, BAL fluid specimen after washing with 10 ml 0.9% NaCl.

* SLE : systemic lupus erythematosus; SCID : severe combined immunodeficiency; RPGN :rapidly progressive glomerulonephritis; MPA : microscopic polyangitis; MG : myasthenia gravis; CRF : chronic renal failure; SVC syndrome : superior vena cava syndrome; PN : polyarteritis nodosa; MVR :mitral valve replacement

TABLE 2.
Comparison of each parameters in non-PCPpatinents

case	sample species	primary disease	age (year)	gender	WBC (/μl) (LYM%)	lymphcyte (/μL)	CRP (mg/dL)	beta-D-glucan (pg/mL) (<11)	Quantitative PCR (PCP)	Quantitative PCR (GAPDH)	(PCP/GAPDH)
1	BAL-100	RPGN/MPA	60	F	5900(14)	826	4.8	92.3	9.19×10^{4}	1.18×10^{6}	<0.1
2	Sputum	MPGN/nephrotic syn./Pulmonary emphysema	74	M	6000(1)	60	9.7	4.4	1.31×10^{8}	2.96×10^{8}	0.4
3	Sputum	RA/RAlung(UIP)/pulmonary emphysema	62	M	13100(25)	3275	1.4	12.3	6.12×10^{7}	1.28×10^{8}	0.5
4	BAL-20	Lung cancer/DiabetesMellitus (type2)/CH-C	67	M	6300(8)	504	0.1	5	5.77×10^{0}	5.09×10^{6}	<0.1
5	Sputum	Lung cancer	56	M	1100(14)	154	1.2	not done	5.21×10^{5}	1.66×10^{6}	0.3

* BAL-100, BAL fluid specimen after washing with 100 ml 0.9% NaCl; BAL-20, BAL fluid specimen after washing with 20 ml 0.9% NaCl; BAL-10, BAL fluid specimen after washing with 10 ml 0.9% NaCl.
* RPGN:rapidly progressive glomerulonephritis; MPA : microscopic polyangitis; MPGN : membranoproliferative glomerulonephritis; RA : Rheumatoid Arthritis; UIP : usual interstitial pneumonia; CH-C: chronic hepatitis C

positive (Table 1 and Table 2). This may have influenced our results. We believe that, in BAL samples, normalization using GAPDH is not useful for the diagnosis of *Pneumocystis* pneumonia. On the other hand, for HIV negative patients, BAL specimens are recommended rather than sputum specimens for the diagnosis of *Pneumocystis* pneumonia by quantitation with real-time PCR.

Patient profiles (Table 1 and Table 2)

The 22 specimens examined in this study were divided into two groups, PCP and non-PCP patients. No difference between the two groups regarding sample species (sputum and BAL) was demonstrated, and they were therefore analyzed together. There were no significant differences in any parameter (sample specimen/primary diseases without HIV/WBC/lymphocyte/CRP/beta-D-glucan) between the PCP and non-PCP patients. When separated according to sample specimens (sputum and BAL), none of the parameters (WBC/lymphocyte/CRP/beta-D-glucan) were significantly different between the PCP and non-PCP patients. In the case of *Pneumocystis* pneumonia, it will be difficult to reach a definitive diagnosis based solely on the patient's clinical condition and laboratory data.

The present study indicated that normalization using GAPDH might be not helpful. However, more studies will be needed to distinguish between PCP, subclinical infection or colonization, and to determine cut-off values for each.

REFERENCES

1. Atzori C, Agostoni F, Angeli E, Mainini A, and Orlando G. Combined use of blood and oropharyngeal samples for noninvasive diagnosis of *Pneumocystis carinii* pneumonia using the polymerase chain reaction. Eur J Clin Microbiol Infect Dis 1998; 17:241-246.
2. Caliendo AM, Hewitt PL, Allega JM, Keen A, Ruoff KL et al. Performance of a PCR assay for detection of *Pneumocystis carinii* from respiratory specimens. J Clin Microbiol 1998; 36:979-982.
3. Cartwright CP, Nelson NA, and Gill VJ. Development and evaluation of a rapid and simple procedure for detection of *Pneumocystis carinii* by PCR. J Clin Microbiol 1994; 32:1634-1638.
4. Chouaid C, Roux P, Lavard I, Poirot JL, and Housset B. Use of the polymerase chain reaction technique on induced-sputum samples for the diagnosis of *Pneumocystis carinii* pneumonia in HIV-infected patients. A clinical and cost-analysis study. Am J Clin Pathol 1995; 104:72-75.
5. Flori P, Bellete B, Durand F, Raberin H, Cazorla C et al. Comparison between real-time PCR, conventional PCR and different staining techniques for diagnosing *Pneumocystis jiroveci* pneumonia from bronchoalveolar lavage specimens. J Med Microbiol 2004; 53:603-607.
6. Geckler RW, Gremillion DH, McAllister CK, and Ellenbogen C. Microscopic and bacteriological comparison of paired sputa and transtracheal aspirates. J Clin Microbiol 1977; 6:396-399.
7. Hauser PM, Blanc DS, Bille J, Nahimana A, and Francioli P. Carriage of *Pneumocystis carinii* by immunosuppressed patients and molecular typing of the organisms. Aids 2000; 14:461-463.
8. Helweg-Larsen J, Jensen JS, Benfield T, Svendsen UG, Lundgren JD et al. Diagnostic use of PCR for detection of *Pneumocystis carinii* in oral wash samples. J Clin Microbiol

1998; 36:2068-2072.
9. Helweg-Larsen J, Jensen JS, Dohn B, Benfield TL, and Lundgren B. Detection of *Pneumocystis* DNA in samples from patients suspected of bacterial pneumonia- a case-control study. BMC Infect Dis 2002; 2:28.
10. Hirooka T, Higuchi T, Tanaka N, and Ogura T. [The value of proper sputum collection instruction in detection of acid-fast bacillus]. Kekkaku 2004; 79:33-37. (in Japanese)
11. Honda J, Hoshino T, Natori H, Tokisawa S, Akiyoshi H et al. Rapid and sensitive diagnosis of cytomegalovirus and *Pneumocystis carinii* pneumonia in patients with haematological neoplasia by using capillary polymerase chain reaction. Br J Haematol 1994; 86:138-142.
12. Huang SN, Fischer SH, O'Shaughnessy E, Gill VJ, Masur H et al. Development of a PCR assay for diagnosis of *Pneumocystis carinii* pneumonia based on amplification of the multicopy major surface glycoprotein gene family. Diagn Microbiol Infect Dis 1999; 35:27-32.
13. Kovacs JA, Ng VL, Masur H, Leoung G, Hadley WK et al. Diagnosis of *Pneumocystis carinii* pneumonia: improved detection in sputum with use of monoclonal antibodies. N Engl J Med 1988; 318:589-593.
14. Larsen HH, Masur H, Kovacs JA, Gill VJ, Silcott VA et al. Development and evaluation of a quantitative, touch-down, real-time PCR assay for diagnosing *Pneumocystis carinii* pneumonia. J Clin Microbiol 2002; 40:490-494.
15. Leigh TR, Kangro HO, Gazzard BG, Jeffries DJ, and Collins JV. DNA amplification by the polymerase chain reaction to detect sub-clinical *Pneumocystis carinii* colonization in HIV-positive and HIV-negative male homosexuals with and without respiratory symptoms. Respir Med 1993; 87:525-529.
16. Leigh TR, Wakefield AE, Peters SE, Hopkin JM, and Collins JV. Comparison of DNA amplification and immunofluorescence for detecting *Pneumocystis carinii* in patients receiving immunosuppressive therapy. Transplantation 1992; 54:468-470.
17. Lipschik GY, Gill VJ, Lundgren JD, Andrawis VA, Nelson NA et al. Improved diagnosis of *Pneumocystis carinii* infection by polymerase chain reaction on induced sputum and blood. Lancet 1992; 340:203-206.
18. Maskell NA, Waine DJ, Lindley A, Pepperell JC, Wakefield AE et al. Asymptomatic carriage of *Pneumocystis jiroveci* in subjects undergoing bronchoscopy: a prospective study. Thorax 2003; 58:594-597.
19. Nevez G, Raccurt C, Jounieaux V, Dei-Cas E, and Mazars E. *Pneumocystosis* versus pulmonary *Pneumocystis carinii* colonization in HIV-negative and HIV-positive patients. Aids 1999; 13:535-536.
20. Olsson M, Elvin K, Lofdahl S, and Linder E. Detection of *Pneumocystis carinii* DNA in sputum and bronchoalveolar lavage samples by polymerase chain reaction. J Clin Microbiol 1993; 31:221-226.
21. Rabodonirina M, Raffenot D, Cotte L, Boibieux A, Mayencon M et al. Rapid detection of *Pneumocystis carinii* in bronchoalveolar lavage specimens from human immunodeficiency virus-infected patients: use of a simple DNA extraction procedure and nested PCR. J Clin Microbiol 1997; 35:2748-2751.
22. Ribes JA, Limper AH, Espy MJ, and Smith TF. PCR detection of *Pneumocystis carinii* in bronchoalveolar lavage specimens: analysis of sensitivity and specificity. J Clin Microbiol 1997; 35:830-835.
23. Roux P, Lavrard I, Poirot JL, Chouaid C, Denis M et al. Usefulness of PCR for detection of *Pneumocystis carinii* DNA. J Clin Microbiol 1994; 32:2324-2326.
24. Sing A, Roggenkamp A, Autenrieth IB, and Heesemann J. *Pneumocystis carinii* carriage in immunocompetent patients with primary pulmonary disorders as detected by single or nested PCR. J Clin Microbiol 1999; 37:3409-3410.
25. Sing A, Trebesius K, Roggenkamp A, Russmann H, Tybus K et al. Evaluation of diagnostic value and epidemiological implications of PCR for *Pneumocystis carinii* in different immunosuppressed and immunocompetent patient groups. J Clin Microbiol 2000; 38:1461-1467.
26. Skot J, Lerche AG, Kolmos HJ, Nielsen JO, Mathiesen LR et al. *Pneumocystis carinii* in bronchoalveolar lavage and induced sputum: detection with a nested polymerase chain reaction. Scand J Infect Dis 1995; 27:363-367.
27. Takahashi T, Goto M, Endo T, Nakamura T, Yusa N et al. *Pneumocystis carinii* carriage in immunocompromised patients with and without human immunodeficiency virus infection. J Med Microbiol 2002; 51:611-614.
28. Torres J, Goldman M, Wheat LJ, Tang X, Bartlett MS et al. Diagnosis of *Pneumocystis carinii* pneumonia in human immunodeficiency virus-infected patients with polymerase chain reaction: a blinded comparison to standard methods. Clin Infect Dis 2000; 30:141-145.
29. Wakefield AE, Guiver L, Miller RF, and Hopkin JM. DNA amplification on induced sputum samples for diagnosis of *Pneumocystis carinii* pneumonia. Lancet 1991; 337:1378-1379.
30. Wakefield AE, Miller RF, Guiver LA, and Hopkin JM. Oropharyngeal samples for detection of *Pneumocystis carinii* by DNA amplification. Q J Med 1993; 86:401-406.
31. Wakefield AE, Pixley FJ, Banerji S, Sinclair K, Miller RF et al. Detection of *Pneumocystis carinii* with DNA amplification. Lancet 1990; 336:451-453.
32. Weig M, Klinker H, Bogner BH, Meier A, and Gross U. Usefulness of PCR for diagnosis of *Pneumocystis carinii* pneumonia in different patient groups. J Clin Microbiol 1997; 35:1445-1449.
33. Zaman MK, Wooten OJ, Suprahmanya B, Ankobiah W, Finch PJ et al. Rapid noninvasive diagnosis of *Pneumocystis carinii* from induced liquefied sputum. Ann Intern Med 1988; 109:7-10.

Original Contribution

Kurume Medical Journal, 55, 63-69, 2008

Bilateral Neurovascular Bundles Sparing Prostatectomy Preserves Sexual Function in Patients with Localized Prostate Cancer

MAKOTO NAKIRI, MASANORI NOGUCHI, TATSUYA ISHITAKE*
AND KEI MATSUOKA

Departments of Urology and Environmental Medicine, Kurume University School of Medicine, Kurume 830-0011, Japan*

Received 8 January 2009, accepted 16 February 2009

Summary: The influence of the presence or absence of the neurovascular bundles on patient QOL were examined using the UCLA Prostate Cancer Index (UCLA-PCI) in patients who underwent radical retropubic prostatectomy. The study was performed in 105 patients who were histopathologically diagnosed with prostate cancer and underwent radical retropubic prostatectomy (During prostatectomy, the bilateral neurovascular bundles were preserved in 45 patients (42.8%), unilateral neurovascular bundle preservation was achieved in 24 (22.9%), and no neurovascular bundles were preserved in 36 (34.2%)). The QOL was evaluated before and after surgery using the Japanese edition of the UCLA-PCI, which examines 6 items. Our findings suggested that 'urinary function, 'urinary bother', 'bowel function', and 'bowel bother' deteriorated early after surgery, and recovered to the preoperative levels in the late phase after surgery, but no significant difference was noted in the time-course among the three groups. In contrast, 'sexual function' was significantly improved in the late postoperative phase only in the bilateral nerve-spared group, but not in the unilateral nerve-spared and non-nerve-spared groups. Patients complaining of 'Sexual bother' were more prevalent in the unilateral nerve-spared group in the late postoperative phase, but the difference was not significant. On multiple regression analysis of factors associated with sexual function in the late postoperative phase, only bilateral nerve preservation of was significantly associated with sexual function in the late postoperative phase ($p<0.0001$). In order to maintain sexual function following radical retropubic prostatectomy, the bilateral neurovascular bundles should be preserved, as far as practicable.

Key words nerve preservation, prostate cancer, QOL, radical retropubic prostatectomy, sexual function, UCLA-Prostate Cancer Index

INTRODUCTION

Prostate cancer is a rare cancer with regard to the concept of course observation without treatment. Considering its characteristic slow growth, the induction of severe, prolonged complications following surgery raises questions doubt the suitability of surgical treatment as compared to radiotherapy, and physicians have to obtain detailed informed consent before surgery, covering the possible occurrence and duration of complications, surgical procedure, and adverse effects.

Detection of localized prostate cancer has markedly increased in recent years with the spread of PSA screening, and radical retropubic prostatectomy is the global standard procedure, taking into consideration patient age and cancer stage. However, this procedure causes complications, such as dysuria (urinary incontinence) and sexual dysfunction (impotence), markedly impairing the patient's QOL in many cases. Of these complications, approaches to postoperative recovery from dysuria (urinary incontinence) have become consistent internationally. Hamada et al. reported that urination is in the recovery period 3

Corresponding Author: Makoto Nakiri, Department of Urology, Kurume University School of Medicine, 67 Asahi-machi, Kurume 830-0011, Japan. Tel: 0942-31-7552 Fax: 0942-31-4370 E-mail: mnakiri@med.kurume-u.ac.jp

Abbreviations: MAB, maximum androgen blockade; UCLA-PCI, UCLA Prostate Cancer Index.

months after surgery, and returned to the preoperative level 6 months after surgery [1], indicating that recovery in the early postoperative phase can be expected. Our hospital has succeeded in early catheter removal, improvement of urinary incontinence, and discharge using Noguchi's anastomosed site-lifting method and by developing a clinical path [2]. In contrast, sexual dysfunction (impotence) occurs in more than half of patients after surgery, and their QOL is impaired for a long time after surgery. The outcome markedly varies among facilities, and at present no standard, consistent approach to preservation of sexual function has been developed, despite the many studies on the influence of nerve-sparing and age on postoperative sexual function that have been published after Walsh et al. initially reported nerve-sparing radical prostatectomy [3].

The UCLA Prostate Cancer Index (UCLA-PCI) is a localized prostate cancer-targeted QOL questionnaire widely used internationally, consisting of 20 items covering 6 aspects of complications following radical prostatectomy ('urinary function', 'urinary bother', 'bowel function', 'bowel bother', 'sexual function', and 'sexual bother'), and the reliability and validity of the Japanese edition has been confirmed [4]. In addition to the disease-targeted QOL questionnaire, FACT-P, EORTC, and SF-36 are generally used as health-related QOL questionnaires in other studies on QOL, but the UCLA-PCI covers typical complications following radical prostatectomy, and consists of only 20 items so is considered less stressful than other indices.

In this study, we evaluated the QOL of patients following radical retropubic prostatectomy for localized prostate cancer using the Japanese edition (version 1.2) of the UCLA-PCI, and investigated the influence of surgery on the patients' QOL, factors involved, changes in the QOL during the postoperative period, and the influence of preservation of the neurovascular bundles, hoping that the findings would prove useful information to patients considering radical prostatectomy.

SUBJECTS AND METHODS

The study was performed in 105 patients who were histopathologically diagnosed with prostate cancer and who underwent radical retropubic prostatectomy at Kurume University Hospital and 8 related facilities between January 2002 and February 2006. The neurovascular bundles were preserved in 69 patients (65.7%) (bilateral: 45 (42.9%), unilateral: 24 (22.9%)), and no nerves were preserved in 36 (34.3%). Regarding nerve preservation, patient's requests were given a high priority, but in most cases the side positive on biopsy was resected. The bilateral nerves were resected in all cases that received concomitant MAB treatment. The localization of cancer in the prostate was confirmed by MRI. As a rule, the bilateral nerves were preserved in all cases after August 2005. The bilateral nerves were resected in all cases with concomitant MAB treatment, as a rule. The same operator performed all surgeries, employing the anastomosed site-lifting method via the retropubic approach developed by Noguchi [2]. The clinical stage was diagnosed following the 5th edition of the TNM classification revised by the UICC in 1997. No postoperative adjuvant therapy, such as treatment with sildenafil citrate, was performed in any patient.

For evaluation of QOL before and after surgery, the Japanese edition (version 1.2) of the UCLA-PCI was used. The patients filled in the questionnaire privately, in the absence of physicians. The survey was performed before surgery and 1, 3, 6, and 12 months after surgery.

One and 3 months after surgery were designated as early postoperative phase, and 6 and 12 months after surgery was the late postoperative phase. In patients who could be surveyed in both phases, answers at 1 month were adopted as those in the early postoperative phase, and answers at 12 months as those in the late postoperative phase in the investigation of time-course changes. Complications were classified into 6 aspects following the international criteria: 'urinary function', 'urinary bother', 'bowel function', 'bowel bother', 'sexual function', and 'sexual bother', and were assessed by assigning a grade from 0 (worst) to 100 (best). In addition, the influence of preserving or not preserving the neurovascular bundles were investigated.

For comparison among the three different nerve-spared groups, one-way ANOVA and chi-square tests were used. Repeated measures ANOVA was performed for comparison of changes in the time-course UCLA-PCI among the different nerve-spared groups. Multiple regression analysis (stepwise method) was employed to investigate factors determining sexual function in the late postoperative phase. A significance level of less than 5% was regarded as significant. Statistical analysis software (JMP version 7.0) was used.

RESULTS

Characteristics of patients by nerve preservation

The characteristics of patients with and without nerve preservation are presented in Table 1. Significant differences were only observed in the preoperative PSA level and operation time. For the clinical stage which divided into those with localized (T1/T2) and non-localized (T3/T4) cases. Many patients in the non-spared group (T3-4: 11) had lesions that were not localized, while only one T3-4 case was present in the unilateral nerve-spared group, showing a significant difference ($p<0.001$). On the preoperative UCLA-PCI survey there was no significant difference in any of the indices among the three different groups.

Changes in UCLA-PCI in groups with and without nerve preservation

Time-course changes in urinary function (A) and bother (B) in groups with and without nerve preservation (Fig. 1): Regarding 'urinary function', there was no significant difference in the preoperative values. In the early postoperative phase, the value deteriorated in the bilateral nerve-spared group, but recovered to the preoperative level in the late postoperative phase. 'Urinary bother' slightly increased with changes in 'urinary function' in the early postoperative phase in all 3 groups, compared to that before surgery, but improved to a level higher than the preoperative value in the late postoperative phase. However, these time-course changes or differences among the groups were not significant.

TABLE 1.
Characteristics of Patients by Group

		Preservation of nerves Total (n=105)			Statistics
		none (n=36)	unilateral (n=24)	bilateral (n=45)	
Age (year)		67.7	66.6	66.8	n.s.
Pre-operative PSA (ng/ml)		13.9	16.1	9.5	p=0.003
Clinical Stage (before treatment of MAB)	T1-2	25	23	45	p<0.001
	T3-4	11	1	0	
No. of MAB		13	3	3	
Operation Time (min)		165.9	166.2	150.5	p=0.023
Blood Loss (ml)		480.8	444.5	457.1	n.s.
Histological Differentiation	well	5	2	11	n.s.
	moderately	23	19	24	
	poorly	1	1	5	
Pathological Stage	T0-1	4	2	4	n.s
	T2	27	17	30	
	T3	0	5	8	
UCLA-PCI scale (pre-operative)	Urinary function	93.9	89.7	86.8	n.s.
	Urinary bother	84.7	90.6	87.8	n.s.
	Bowel function	92.1	95.8	89.7	n.s.
	Bowel bother	93.8	94.8	94.9	n.s.
	Sexual function	24.9	38.9	34.0	n.s.
	Sexual bother	77.1	79.2	73.3	n.s.

Some data on histological differentiation and pathological stage were not available. n.s.: not significant

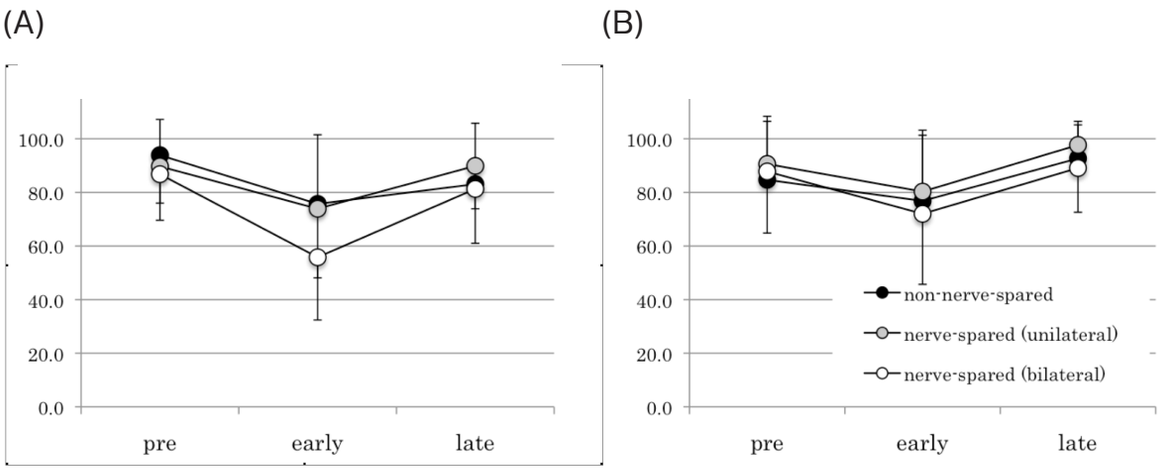

Fig. 1. Time-course changes in urinary function (A) and urinary bother (B) by nerve preservation. Urinary function and urinary bother were assessed by assigning a grade from 0 (worst) to 100 (best). Points of each symbol and vertical bar (one-side) indicate means and standard deviations, respectively.

Time-course changes in bowel function (A) and bother (B) in groups with and without nerve preservation (Fig. 2): Both 'bowel function' and 'bowel bother' slightly deteriorated in the early postoperative phase with or without nerve preservation, but recovered to the preoperative levels by the late postoperative phase in all three groups. There were no significant differences in the time-course changes between the groups.

Time-course changes in sexual function (A) and bother (B) in groups with and without nerve preservation (Fig. 3): Regarding 'sexual function', there were no preoperative differences among the three groups. In the early postoperative phase the mean scores dramatically decreased in all 3 groups, showing a marked impairment of the QOL. In the late postoperative phase, recovery was favorable in the bilateral nerve-spared group, but poor in the unilateral nerve-spared group as well as the non-nerve-spared group. The time-course changes in sexual function showed significant differences among the three groups (p=0.0015 on repeated-measures ANOVA). Regarding 'sexual bother', no aggravation was noted in the early postoperative phase in the non-nerve-spared group. In the nerve-spared group, despite an improved QOL score for 'sexual function', bother deteriorated in the late postoperative phase in the unilateral nerve-spared group, but the time-course change was not sig-

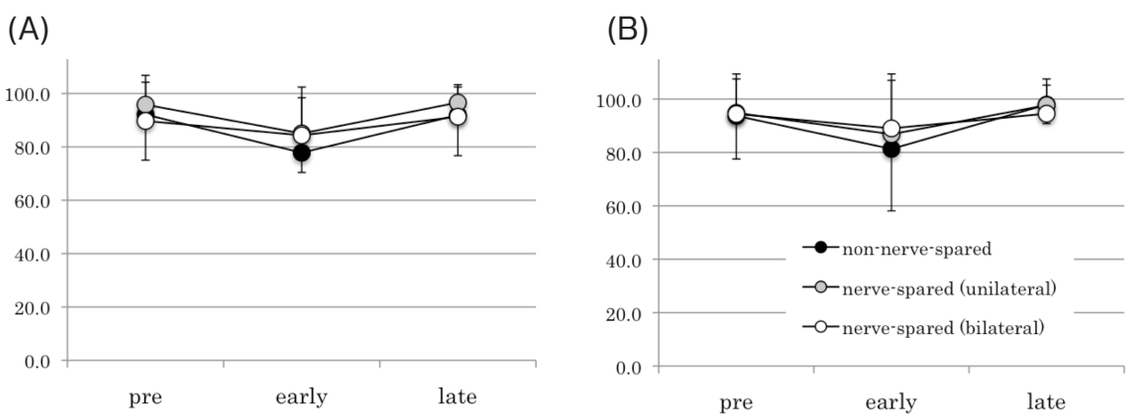

Fig. 2. Time-course changes in bowel function (A) and bowel bother (B) by nerve preservation. Bowel function and bowel bother were assessed by assigning a grade from 0 (worst) to 100 (best). Points of each symbol and vertical bar (one-side) indicate means and standard deviations, respectively.

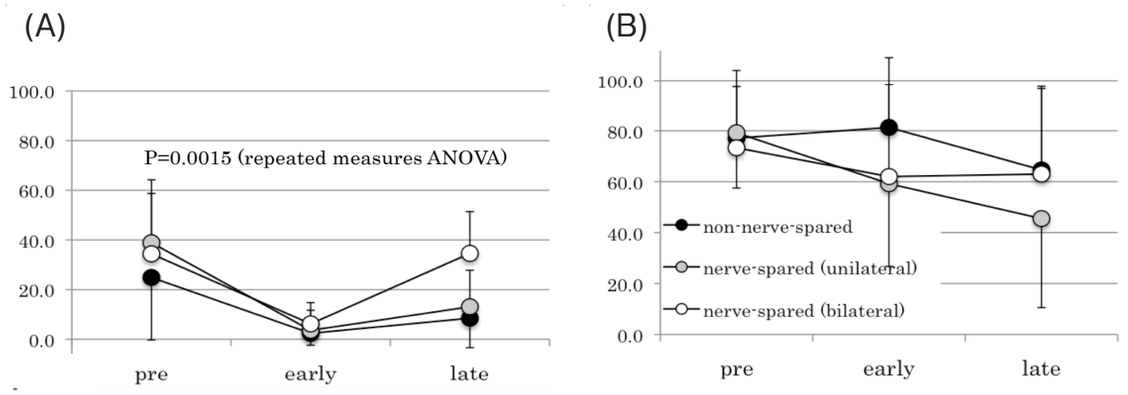

Fig. 3. Time-course changes in sexual function (A) and sexual bother (B) by nerve preservation. Sexual function and sexual bother were assessed by assigning a grade from 0 (worst) to 100 (best). Points of each symbol and vertical bar (one-side) indicate means and standard deviations, respectively.

nificant.

Multiple regression analysis of sexual function

Of the measured indices of the UCLA-PCI, a significant difference was noted in 'sexual function' in the late postoperative phase between the nerve-spared and non-spared groups. This finding was subjected to multiple regression analysis (stepwise method) regarding age, preoperative PSA level, operation time, blood loss, clinical stage (categorized into 2 stages), presence or absence of nerve preservation, and preoperative value of sexual function (on the UCLA-PCI scale) as explanatory variables. Nerve preservation and preoperative sexual function value (on the UCLA-PCI scale) remained in the final model (Table 2). Only bilateral nerve preservation was significantly associated with sexual function in the late postoperative phase ($p<0.0001$), whereas unilateral nerve preservation showed no association ($p=0.0653$).

TABLE 2.
Multiple Regression Analysis (UCLA-PCI Scale) of Late Postoperative Sexual Function

	Parameter estimate	Standard error	p value
Nerve-spared [unilateral]	−6.033	3.206	0.0653
[bilateral]	15.443	2.658	<0.0001
Pre-operative sexual function	0.124	0.0735	0.098

Multiple regression analysis was performed by step-wise method (forward selection) for 7 variables (age, preoperative PSA level, operation time, blood loss in operation, clinical stage, nerve preservation and preoperative value of sexual function).

DISCUSSION

Changes in the QOL following retropubic prostatectomy for localized prostate cancer were prospectively investigated using the UCLA-PCI. The UCLA-PCI items 'urinary function', 'urinary bother', 'bowel function', and 'bowel bother', tended to deteriorate in the early postoperative phase (1-3 months after surgery), but recovered to the preoperative levels in the late postoperative phase (6-12 months after surgery), and there were no significant differences in the time-course changes between the nerve-spared and non-spared groups. Regarding 'sexual function', the value on the QOL scale decreased in the early postoperative phase in both groups, but recovered in the late postoperative phase only in the nerve-spared group, showing a significant improvement of sexual function compared to that in the non-nerve-spared group. On multiple regression analysis to investigate factors associated with sexual function in the late postoperative phase, only the presence or absence of spared nerve showed a significant association.

Since Walsh et al. initially reported nerve-sparing radical prostatectomy [3], there have been many reports on sexual function following this surgery. Quinlan et al. surveyed patients with preoperative capability of sexual intercourse at least 18 months after surgery in a single facility, and found that 68% had sufficient potency for sexual intercourse [5]. In the study reported by Walsh et al., potency recovered in

73% of patients after 12 months and 86% after 18 months, showing favorable outcomes [6]. Catalona et al. reported that recovery of potency was favorable in young patients who underwent bilateral nerve-sparing surgery [7]. However, Litwin et al. reported that there was no difference in postoperative sexual function between patients with and without application of nerve-sparing [8]. Furthermore, Talcott et al. reported that recovery of postoperative potency in nerve-spared patients were less than previously reported [9]. With regard to the favorable outcomes achieved by Walsh et al., 1/3 of their patients were treated with Viagra (sildenafil), and it was pointed out that patient selection was involved in the outcome of recovered sexual function [8,9]. In a review of sexual function following radical prostatectomy reported by Dubbelman et al., the rate of patients with potency following bilateral nerve-sparing radical prostatectomy was within a range of 31-86%, and the number of spared nerves, age, and preoperative sexual activity were the most important factors for the recovery of potency [10]. There is a marked variation in potency following nerve-sparing surgery among facilities, as shown above. Regarding the cause for this variation, Walsh et al. assumed that the variation was due to the weight of excised specimen, experience of the surgeon, and age and health condition of patients [6]. We analyzed factors associated with sexual function in the late postoperative phase by multiple regression analysis, and found no association with age, operation time, blood loss, preoperative PSA level, clinical stage (categorized into 2 stages), or preoperative value of sexual function on the UCLA-PCI scale. Only nerve sparing was significantly associated with sexual function. However, a marked difference due to the number of spared nerves (unilateral or bilateral) was noted, as reported by Dubbelman et al. Regarding this point, Noldus et al. [11] reported that recovery of sexual function was significantly more favorable in the bilateral nerve-spared than in the unilateral nerve-spared group. Rabbani et al. [12] also reported that the number of spared nerves was an influential factor for the postoperative recovery of sexual function.

Nerve preservation is an important factor in consideration of patients' QOL following radical prostatectomy, and this study clarified that bilateral nerve sparing is desirable. Nerve-sparing is an important independent factor for the recovery of sexual function following radical prostatectomy, separate from the other factors, such as age and preoperative sexual function, supporting the recommendation of nerve-sparing surgery, but it may be wise to use electric stimulation to accurately judge the feasibility of nerve-sparing. The results of this study may be useful in explaining surgical procedures and the effects of radical prostatectomy to patients.

We used the UCLA-PCI for the QOL questionnaire. The UCLA-PCI is a disease-targeted QOL questionnaire, covering 'urinary function', 'urinary bother', 'bowel function', 'bowel bother', 'sexual function', and 'sexual bother' as typical complications following radical prostatectomy. It is simple, consisting of only 20 items, and requires little time or effort on the part of patients, so it is less stressful than other indices [4]. However, QOL factors other than sexual function may also determine the recovery of potency, as Litwin et al. reported that sexual function was impaired by the presence of urinary incontinence in 20% of patients who underwent surgery [8]. Moreover, inconvenience in daily life, not only the age of the patient but also the age and sexual activity of his partner, and patient's mental stress may affect sexuality and potency. Thus, for the assessment of postoperative sexual function, the QOL should be comprehensively evaluated in various aspects by concomitantly employing FACT-P, EORTC, and SF-36 as general health-related QOL questionnaires.

Distress tended to increase in the late postoperative phase in the unilateral nerve-spared group. The patients may have been anxious about when their function would recover to the preoperative level, or may have had unrealistic expectation for the spared nerve due to inadequate explanation before surgery of the likelihood of recovery of sexual function by unilateral nerve-sparing. This was a matter of concern regarding the suitability of radical prostatectomy for localized prostate cancer, reconfirming that changes in the QOL after surgery should be considered in the evaluation of the prognosis, and detailed information concerning sexual function, including possible changes in the QOL after surgery should be provided to patients before surgery.

On the UCLA-PCI scale, the value of sexual function was 32.2 before surgery, and those in the early and late postoperative phases were 4.0 and 19.7, respectively. These were markedly lower than those in patients following open radical prostatectomy reported by Ball et al. [13], where sexual function on the UCLA-PCI was 59 before surgery, and 19, 24, and 33 at 1, 3, and 6 months after surgery. These differences may reflect the fact that reduced sexual function and activity is not regarded as so important in the daily life of the elderly in Japan as it seems to be in Western countries. It is also implied that differences

in ways of thinking or habits concerning sex between Europeans/Americans and Japanese may be involved. Since there have been no reports concerning Japanese sexual culture, further assessment of the QOL with regard to 'sex' in Japanese may be necessary.

REFERENCES

1. Hamada Y, Kitani K, Kawano T, Otsuka Y, Sasho K et al. Assessment of quality of life in men treated for localized prostate cancer: before and after radical prostatectomy. Nishinihon J Urol 2004; 66:241-248.
2. Noguchi M, Shimada A, Yahara J, Suekane S, and Noda SA. Early catheter removal 3 days after radical retropubic prostatectomy. Int J Urol 2004; 11:983-988.
3. Walsh PC, and Donker PJ. Impotence following radical prostatectomy: insight into etiology and prevention. J Urol 1982; 128:492-497.
4. Suzukamo Y, Kakei Y, Kamamoto T, Arai Y, Ogawa O et al. Translation and adaptation of the UCLA Prostate Cancer Index for use in Japan. Jpn J Urol 2002; 93:659-668. (in Japanese)
5. Quinlan DM, Epstein JI, Carter BS, and Walsh PC. Sexual function following radical prostatectomy: Influence of preservation of neurovascular bundles. J Urol 1991; 145:998-1002.
6. Walsh PC, Marschke P, Ricker D, and Burnett AL. Patient-reported urinary continence and sexual function after anatomic radical prostatectomy. Urology 2000; 55:58-61.
7. Catalona WJ, Carvalhal GF, Mager DE, and Smith DS. Potency, continence and complication rates in 1,870 consecutive radical retropubic prostatectomies. J Urol 1999; 162:433-438.
8. Litwin MS, Hays RD, Fink A, Ganz PA, Leake B et al. Quality-of-life outcomes in men treated for localized prostate cancer. JAMA 1995; 273:129-135.
9. Talcott JA, Rieker P, Propert KJ, Clark JA, Wishnow KI et al. Patient-reported impotence and incontinence after nerve-sparing radical prostatectomy. J Natl Cancer Inst 1997; 89:1117-1123.
10. Dubbelman YD, Dohle GR, and Schroder FH. Sexual function before and after radical retropubic prostatectomy: A systematic review of prognostic indicators for a successful outcome. Eur Urol 2006; 50:711-720.
11. Noldus J, Michl U, Graefen M, Haese A, Hammerer P et al. Patient-reported sexual function after nerve-sparing radical retropubic prostatectomy. Eur Urol 2002; 42:118-124.
12. Rabbani F, Stapleton AM, Kattan MW, Wheeler TM, and Scardino PT. Factors predicting recovery of erections after radical prostatectomy. J Urol 2000; 164:1929-1934.
13. Ball AJ, Gambill B, Fabrizio MD, Davis JW, Given RW et al. Prospective longitudinal comparative study of early health-related quality-of-life outcomes in patients undergoing surgical treatment for localized prostate cancer : A short-term evaluation of five approaches from a single institution. J Endourol 2006; 20:723-731.

Original Contribution

Kurume Medical Journal, 55, 71-75, 2008

Is Antiplatelet Therapy for the Prevention of Ischemic Stroke Associated with the Prognosis of Intracerebral Hemorrhage?

AKIRA ISHIBASHI, YOSHITAKE YOKOKURA* AND HISASHI ADACHI**

Departments of Neurosurgery and Surgery, Yokokura Hospital, Fukuoka 839-0215,*
***Department of Medicine, Kurume University School of Medicine,*
Kurume 830-0011, Japan

Received 20 January 2009, accepted 9 March 2009

Edited by TAKASHI OKAMURA

Summary: To examine whether antiplatelet therapy contributes to the unfavorable prognosis of intracerebral hemorrhage, we enrolled 253 consecutive patients (120 men and 133 women; 72.9±11.7 years) hospitalized in our institution within 24 hrs after onset of intracerebral hemorrhage. The location and size of intracerebral hemorrhage were determined from computed tomography (CT). Hematoma enlargement was identified on the basis of a second computed tomography scan performed on the day after admission. An unfavorable prognosis was defined as an outcome of worsening or death using the modified Rankin Scale (mRS).

Locations of intracerebral hemorrhage (ICH) determined from CT were the thalamus in 92 patients (36.3%), putamen in 79 (31.2%), subcortex in 35 (13.8%), cerebellum in 20 (7.9%), brainstem in 18 (7.1%), and caudate nucleus in 9 (3.5%). Sizes of ICH were small and moderate in 153 patients (60%) and large in 100 (40%). Seventeen patients (6.7%) received antiplatelet therapy for stroke prevention. Hematoma enlargement was identified in 39 patients (15.4%). Overall outcomes at the time of discharge were unfavorable (modified Rankin Scale score 5-6) in 64 patients (25.2%) and favorable mRS score (0-1~4) in 189 (74.8%). Univariate analysis demonstrated that age $\geq$75 years (odds ratio: 2.78; 95%CI: 1.54-5.04) and presence of a large hematoma (odds ratio: 19.28; 95%CI: 8.84-42.1) were significantly related to the unfavorable prognosis. Using multiple logistic regression analysis after adjustments for age and sex, the presence of a large hematoma was still judged unfavorable; however, antiplatelet therapy was not related to unfavorable prognosis.

Antiplatelet therapy may be unrelated to the unfavorable prognosis of ICH.

Key words intracerebral hemorrhage, antiplatelet therapy, hypertension, computed tomography, ischemic stroke

INTRODUCTION

Recently, antiplatelet therapy has been recognized to be an important therapeutic option for the prevention of secondary ischemic stroke [1]. The Chinese Acute Stroke Trial (CAST) [2] and the International Stroke Trial (AST) [3] revealed that prompt daily use of aspirin is beneficial in patients with acute ischemic stroke for reducing the risk of early recurrence. Therefore, aspirin is now widely used to reduce the risk of secondary ischemic stroke [4].

Some studies have suggested that aspirin increases the risk of hemorrhagic stroke [5,6]. Gorelick et al. [5] stated that aspirin is a valuable and cost-effective antiplatelet agent and the benefits of aspirin use are significantly more important than the risk of a major intracerebral hemorrhage (ICH). However, it has not well been documented whether the use of aspirin is related to the unfavorable prognosis of patients with ICH. Therefore, in this article, we retro-

Address for correspondence: Akira Ishibashi MD, Department of Neurosurgery, Yokokura Hospital, 394 Takada-machi, Miyama-city, Fukuoka 839-0215, Japan. Tel: +81 944-22-5811 Fax: +81 944-22-2045

Abbreviations: CT, computed tomography; ICH, intracerebral hemorrhage; IVH, intraventricular hemorrhage; mRS, modified Rankin Scale.

spectively reviewed the available therapy data from medical records to examine whether antiplatelet therapy contributes to the unfavorable prognosis of ICH at the time of hospital discharge.

MATERIALS AND METHODS

We reviewed the records of 253 consecutive patients (120 men and 133 women; age, 72.9±11.7 years) who were hospitalized in our institution within 24 hrs after onset of ICH between January 1998 and September 2007 (Table 1). Aspirin, warfarin, and cilostazol were taken as the antiplatelet/anticoagulation therapy for the prevention of the secondary ischemic stroke. In all patients, the locations and initial sizes of ICH were determined from computed tomography (CT) and classified into subgroups using the CT classification of Kanaya et al. [7] for the putamen and thalamus (Table 2-1, 2). Other locations of ICH were the subcortex, cerebellum, pons, and caudate nucleus. Sizes of hematoma were classified into small, moderate and large in each location (Table 2-1,

TABLE 1.
Baseline characteristics of 253 patients with intracerebral hemorrhage

Characteristics	aspirin (–) (n=221)	Aspirin (+) (n=17)	Aspirin & warfarin (n=5)	warfarin (+) (n=3)	silostazole (+) (n=1)	unknown (n=6)	Total (n=253)
men n=(%)	107 (48%)	7 (41%)	2 (40%)	1 (33%)	1 (100%)	2 (33%)	120 (47%)
Wemen n=(%)	114 (52%)	10 (58.9%)	3 (60%)	2 (67%)	0 (0%)	4 (67%)	133 (53%)
mean age	72.2	78	77.2	79	70	76.6	72.9
Previous Disease							
Hypetension	184 (83%)	11 (64.7%)	2 (40%)	3 (100%)	0 (0%)	1 (16.6%)	201 (79%)
Cardiac disease	15 (6.7%)	5 (29.4%)	4 (80%)	1 (33%)	0 (0%)	3 (50%)	28 (11%)
ischemic storke	19 (8.5%)	11 (64.7%)	0 (0%)	2 (67%)	1 (100%)	0 (0%)	33 (13%)
Hemorrhagic stroke	24 (10.8%)	1 (5.8%)	2 (40%)	0 (0%)	0 (0%)	0 (0%)	27 (10%)
Diabetes mellitus	48 (21.7%)	6 (35.2%)	0 (0%)	1 (%)	1 (100%)	1 (16%)	57 (22%)
Current smoking	52 (23.5%)	1 (5.8%)	0 (0%)	0 (0%)	0 (0%)	1 (16%)	54 (21%)
Liver disease	19 (8.6%)	0 (0%)	0 (0%)	0 (0%)	0 (0%)	0 (0%)	19 (7.5%)

TABLE 2-1.
Computed tomography classification of intracerebral hemorrhage

Putamen		
	Small	localized on the outside of internal capsule
	Moderate	extended to anterior or posterior limb with or without IVH
	Large	extended to anterior and posterior limb with or without IVH
Thalamus		
	Small	localized in the thalamus
	Moderate	extended to internal capsule with or without IVH
	Large	extended to hypothalamus or midbrain with or without IVH
Subcortex		
	Small	＜3cm
	Moderate	3≦ICH＜5cm
	Large	≧5cm

ICH: intracerebral hemorrhage, IVH: intraventricular hemorrhage

TABLE 2-2.
Computed tomography classification of intracerebral hemorrhage

Cerebellum		
	Small	＜3cm
	Moderate	3≦ICH＜5cm
	Large	≧5cm
Brainstem		
	Small & Moderate	hemisphere hematoma
	Large	central portion hematoma
Caudate N.		
	Small	localized in the Caudate N with or without IVH
	Moderate	extended to intemal capsule with or without IVH
	Large	extended to putamen or thalamus with or without IVH

ICH: intracerebral hemorrhage, IVH: intraventricular hemorrhage

2). Hematoma enlargement was defined by its larger size relative to its initial size on a second CT scan performed on the day after admission. The following baseline characteristics were analyzed: age; sex; history of hemorrhagic stroke, ischemic stroke, cardiac disease, or liver disease; current smoking; and hypertension ≥200 mmHg on admission. Daily aspirin use, warfarin treatment, and cilostazol treatment were also assessed as baseline characteristics (Table 1). Univariate and multiple logistic regression analyses were conducted for statistical analysis. The prognosis at the time of hospital discharge was defined as favorable outcome scores of 0-1~4 and unfavorable outcome scores of 5 or 6 using the modified Rankin Scale (mRS) [8].

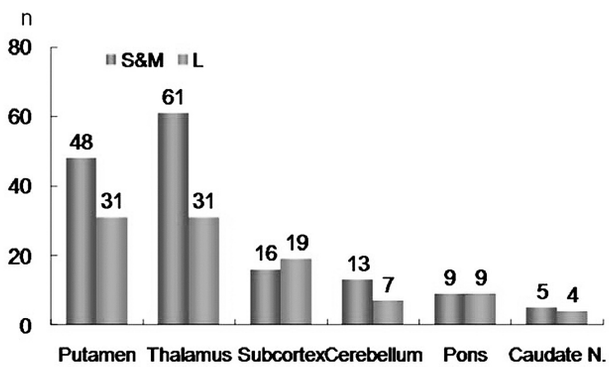

Fig. 1. Size of the hematoma.

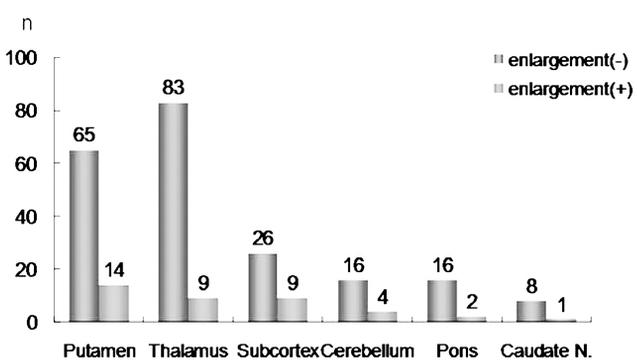

Fig. 2. Enlargement of the hematoma after hospital admission.

RESULTS

Among the 253 patients reviewed, 17 (6.7%) patients were taking aspirin (100 mg) daily before the onset of ICH. Five patients were taking aspirin and warfarin. Three patients were taking warfarin only and 1 patient was taking cilostazol. The locations of ICH determined from CT were the thalamus in 92 patients (36.3%), putamen in 79 (31.2%), subcortex in 35 (13.8%), cerebellum in 20 (7.9%), brainstem in 18 (7.1%), and caudate nucleus in 9 (3.5%). The sizes of ICH were small and moderate in 153 patients (60%) and large in 100 (40%) (Fig. 1). Hematoma enlargement was identified in 39 patients (15.4%) (Fig. 2). Of 17 patients who were taking aspirin, the sizes of ICH were small and moderate in 10 patients (58.8%) and large in 7 (41.2%). Hematoma enlargement was identified in one patient (5.8%). Of 221 patients without antiplatelet therapy, the sizes of ICH were small and moderate in 133 patients (60.2%) and large in 88 (39.8%). Hematoma enlargement was found in 35 pa-

tients (15.9%). Hematoma enlargement was more frequent in those patients without antiplatelete therapy.

The overall outcomes at the time of discharge were unfavorable (mRS score 5-6) in 64 patients (25.2%) and favorable (mRS score 0-1~4) in 189 (74.8%) (Fig. 3). The outcomes of 17 patients who were taking aspirin were unfavorable in 5 patients (29.4%) and favorable in 12 (70.6%). The outcomes of 221 patients without antiplatelet therapy were unfavorable in 56 patients (25.3%) and favorable in 165 (74.7%). The unfavorable outcome in patients who were taking aspirin increased slightly, but this was not statistically significant. Patients' death rates were 0% in patients 35-45 years of age, 6% in patients 45-54 years of age, 12% in patients 55-64 years of age, 12.5% in 65-74 years of age, 23% in patients 75-84 years of age, 32% in patients 85-94 years of age, and 50% in patients ≥95 years. Advanced patient age, especially 75 years or older, was significantly correlated with an unfavorable prognosis.

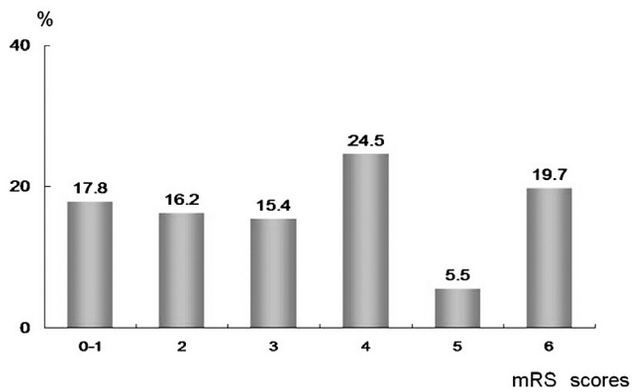

Fig. 3. Outcomes at the time of hospital discharge based on modified Rankin Scale scores.

Of the baseline characteristics, hypertension, cardiac disease, ischemic stroke, hemorrhagic stroke, diabetes mellitus, current smoking, liver disease, and enlargement of the hematoma were not significantly related to an unfavorable prognosis. Univariate analysis demonstrated that patient age ≥75 years (odds ratio: 2.78; 95% CI: 1.54-5.04) and presence of a large hematoma (odds ratio: 19.28; 95% CI: 8.84-42.1) were significantly related to the unfavorable prognosis (Table 3). Using multiple logistic regression analysis after adjustments for age and sex, presence of a large hematoma was still unfavorable (Table 4); however, antiplatelet therapy was not related to unfavorable prognosis.

TABLE 3.
Factors associated with unfavorable prognosis of intracerebral hemorrhage by univariate analysis

Factors	β	SE	p-value
Age	0.053	0.014	<0.001
Age>=75	1.025	0.302	<0.001
Sex	0.198	0.291	0.497
Hematoma (yes)	2.959	0.398	<0.001
Hematoma enlargement (yes)	–0.161	0.411	0.695
HT (yes)	–0.638	0.346	0.065
DM (yes)	–0.064	0.349	0.854
HL (yes)	–0.800	0.468	0.087
Antiplatelet therapy (yes)	0.200	0.554	0.718

HT: Hypertension, DM: Diabetes mellitus, HL: Hyperlipidemia

TABLE 4.
Factors associated with unfavorable prognosis of intracerebral hemorrhage by multiple logistic regression analysis adjusted for age and sex

Factors	β	SE	Odds ratios	95%C. I
Hematoma (yes)	2.890	0.404	17.993	8.159-39.081
Antiplatelet therapy (yes)	–0.055	0.569	0.923	0.310-2.885

DISCUSSION

Aspirin was developed as an antifebrile and analgesic medication almost a century ago. It has been used for primary and secondary prevention of myocardial infarction and ischemic stroke [6]. A recent study reported that 30% of the patients with ICH were taking aspirin [10] and that the use of aspirin therapy was associated with a two-fold increase in the risk of ICH in patients with cerebrovascular diseases [5,6,10]. Therefore, we focused on the effect of antiplatelet therapy on outcomes at the time of hospital discharge of 253 patients with ICH. Of these 253 patients, 17 (6.7%) were taking aspirin. A large hematoma was identified in 100 (40%) of these 253 patients with ICH on an initial CT. We found a significant association between the presence of a large hematoma and the unfavorable prognosis of ICH. Hematoma enlargement after hospital admission was found in 39 (15.4%) patients with ICH, but this enlargement of hematoma made no difference in their prognosis. This implied that a hematoma of sufficient size to cause acute neurological deterioration had already formed before admission. Some studies [1,6,11] stated that antiplatelet therapy was an independent predictor for acute hematoma enlargement and emergent death. Recently, Hanger et al. [12] reported that warfarin was independently associated with an increase in early mortality, but aspirin did not increase the risk of early death. It is unclear from their report, whether aspirin and warfarin were associated with hematoma enlargement after hospital admission, because a second CT scan was not routinely performed. In the present study, antiplatelet therapy was not associated with the formation of a large hematoma contributing to the unfavorable prognosis. Furthermore, there was no statistical correlation between antiplatelet therapy and the unfavorable prognosis of ICH. According to the relationship between patient age and prognosis, patients who were 75 years old or older were more at risk for an unfavorable prognosis than those who were younger. This finding was similar to the previous studies [10,12].

In conclusion, we found a significant association between the presence of a large hematoma and the unfavorable prognosis of ICH. Patients who were 75 years old or older were more at risk for an unfavorable prognosis than those who were younger. Based on our findings, we concluded that there is no statistical correlation between antiplatelet therapy and the unfavorable prognosis of ICH. However, we acknowledge that our series is insufficiently large to draw definitive conclusions about the relationship between antiplatelet therapy and the prognosis of ICH. Larger series of patients are needed to confirm these preliminary data.

ACKNOWLEDGMENTS: We are very grateful to Ms. Seiko Hashimoto for her assistance in preparing the manuscript.

REFERENCES

1. Saloheimo P, Ahonen M, Juvela S, Pyhtinen J, and Savolainen ER. Regular aspirin use preceding the onset of primary intracerebral hemorrhage is an independent predictor for death. Stroke 2006; 37:120-133.
2. CAST (Chinese Acute Stroke Trial) Collaborative Group. CAST: a randomised placebo-controlled trial of early aspirin use in 20,000 patients with acute ischemic stroke. Lancet 1997; 349:1641-1649.
3. International Stroke Trial Collaborative Group. The International Stroke Trial (IST): a randomized trial of aspirin, subcutaneous heparin, both, or neither among 19,435 patients with acute ischemic stroke. Lancet 1997; 349:1569-1581.
4. Chen ZM, Standercock P, Pan HC, Collins R, Liu L et al. Indications for early aspirin use in acute ischemic stroke. A combined analysis of 40,000 patients from the Chinese Acute Stroke Trial and the International Stroke Trial. Stroke 2000; 31:1240-1249.
5. Gorelick PB, and Weisman SM. Risk of hemorrhagic stroke with aspirin use. An update. Stroke 2005; 36:1801-1807.
6. He J, Whelton PK, Brian V, and Klag MJ. Aspirin and the risk of hemorrhagic stroke. JAMA 1998; 280:1930-1935.
7. Kanaya H, Yukawa H, Itoh Z, Kanno T, Kuwabara T et al. A neurological grading for patients with hypertensive intracerebral hemorrhage and a classification of hematoma location on computed tomography: In Proceedings of the 7th Conference of the Surgical Treatment of Stroke, Tokyo. Neuron 1978; 265-270. (in Japanese)
8. Modified Rankin Scale: http://www.strokecenter.org/trials.scales/rankin.html.
9. Toyoda K, Okada Y, Minematu K, Kamouchi M, Fujimoto S et al. Antiplatelet therapy contributes to acute deterioration of intracerebral hemorrhage. Neurology 2005; 65:1000-1004.
10. Rosand J, Eckman MH, Knudsen KA, Singer DE, and Greenberg SM. The effect of warfarin and intensity of anticoagulation on outcome of intracerebral hemorrhage. Arch Intern Med 2004;164:880-884.
11. Hart RG, Tonarelli SB, and Pearce LA. Avoiding central nervous system bleeding during antithrombotic therapy. Recent data and ideas. Stroke 2005; 36:1588-1593.
12. Hanger HC, Fletcher VJ, Wilkinson TJ, Brown AJ, Frampton CM et al. Effect of aspirin and warfarin on early survival after intracerebral haemorrhage. J Neurol 2008; 255:347-352.